

Scheme dependence of two-loop hard thermal loop perturbation theory resummed $\text{SYM}_{4,4}$ thermodynamics

Qianqian Du^{1,2,3} , Michael Strickland⁴ , and Ubaid Tantary⁴

¹*Department of Physics, Guangxi Normal University, Guilin, 541004, China*

²*Guangxi Key Laboratory of Nuclear Physics and Technology, Guilin, 541004, China*

³*Institute of Particle Physics and Key Laboratory of Quark and Lepton Physics (MOS), Central China Normal University, Wuhan, 430079, China*

⁴*Department of Physics, Kent State University, Kent, Ohio 44242, United States*



(Received 18 January 2022; accepted 17 March 2022; published 11 April 2022)

The resummed thermodynamics of $\mathcal{N} = 4$ supersymmetric Yang-Mills theory in four space-time dimensions has been calculated previously to two loop order within hard thermal loop perturbation theory (HTLpt) using the canonical dimensional regularization (DRG) scheme. Herein, we revisit this calculation using the regularization by dimensional reduction (RDR) scheme. Since the RDR scheme manifestly preserves supersymmetry it is the preferred scheme; however, it is important to assess if and by how much the resummed perturbative results depend on the regularization scheme used. Comparing predictions for the scaled entropy obtained using the DRG and RDR schemes we find that for $\lambda \lesssim 6$ they are numerically very similar. We then compare the results obtained in both schemes with the strict perturbative result, which is accurate up to order λ^2 , and a generalized Padé approximant constructed from the known large- N_c weak- and strong-coupling expansions. Comparing the strict perturbative expansion of the two-loop HTLpt result with the perturbative expansion to order λ^2 , we find that both the DRG and RDR HTLpt calculations result in the same scheme-independent predictions for the coefficients at order λ , $\lambda^{3/2}$, and $\lambda^2 \log \lambda$; however, at order λ^2 there is a residual regularization scheme dependence.

DOI: [10.1103/PhysRevD.105.074004](https://doi.org/10.1103/PhysRevD.105.074004)

I. INTRODUCTION

Supersymmetric field theories have generated a great deal of interest in the past decades [1–5]. Such field theories are invariant under supersymmetry transformations in which bosonic and fermionic degrees of freedom are transformed into one another. Although there is currently no experimental evidence that such theories are realized in nature, they have recently proven to be useful due to the ability to employ the conjectured (and strongly evidenced) holographic duality between strongly coupled conformal field theory (CFT) in the large- N_c limit and weakly coupled gravity in five-dimensional anti-de Sitter space (AdS) [6]. This conjectured mathematical equivalence is called the AdS/CFT correspondence and, in the context of thermodynamics, has been used to calculate the strong-coupling limit of $\mathcal{N} = 4$ supersymmetric field theory in four space-time dimensions ($\text{SYM}_{4,4}$) [7]. In this paper, we focus on

resummed perturbative calculations of thermodynamics in $\text{SYM}_{4,4}$ which complement such calculations.

One of the motivations for the calculation presented herein is to test methods that have been applied in the context of finite temperature and density quantum chromodynamics (QCD). In particular, we would like to apply perturbative reorganizations which have been used to improve the convergence of the successive perturbative approximations to the QCD thermodynamic potential [8–29]. These studies have demonstrated that it is possible to obtain excellent agreement with continuum extrapolated lattice calculations of QCD thermodynamics for $T \gtrsim 250\text{--}300$ MeV using such methods. Unlike $\text{SYM}_{4,4}$, QCD is a confining theory at low temperature; however, at high temperature there are many similarities between $\text{SYM}_{4,4}$ and QCD. This stems from the fact that (a) QCD is asymptotically free and (b) the two theories are similar in the weak coupling limit. Comparing perturbative $\text{SYM}_{4,4}$ and QCD one finds that (1) the forms of gluonic and fermionic collective modes are the same, and the scalar collective modes are those of a massive relativistic particle; (2) the transport coefficients, such as the shear viscosity η , which are dominated by the Coulomb-like interactions, are quite similar [30]; and (3) the energy loss and momentum broadening of highly energetic test particles are also alike

Published by the American Physical Society under the terms of the Creative Commons Attribution 4.0 International license. Further distribution of this work must maintain attribution to the author(s) and the published article's title, journal citation, and DOI. Funded by SCOAP³.

[31]. These studies indicate that the key difference between perturbative finite-temperature QCD and $\text{SYM}_{4,4}$ is the number and type of degrees of freedom, with $\text{SYM}_{4,4}$ having, in addition to the adjoint gauge field, four adjoint Majorana fermions and six adjoint scalars.

Unlike QCD, however, $\text{SYM}_{4,4}$ is ultraviolet finite due to its supersymmetric nature and has a vanishing β function. Due to this, the 't Hooft coupling $\lambda = g^2 N_c$ in $\text{SYM}_{4,4}$ does not run and is independent of the temperature. In the weak-coupling limit, the thermodynamics of $\text{SYM}_{4,4}$ has been calculated through order λ^2 with the result being [32–37]

$$\begin{aligned} \frac{\mathcal{F}}{\mathcal{F}_{\text{ideal}}} = \frac{\mathcal{S}}{\mathcal{S}_{\text{ideal}}} &= 1 - \frac{3}{2} \frac{\lambda}{\pi^2} + (3 + \sqrt{2}) \left(\frac{\lambda}{\pi^2} \right)^{3/2} \\ &+ \left[-\frac{21}{8} - \frac{9\sqrt{2}}{8} + \frac{3}{2} \gamma_E + \frac{3}{2} \frac{\zeta'(-1)}{\zeta(-1)} \right. \\ &\left. - \frac{25}{8} \log 2 + \frac{3}{2} \log \frac{\lambda}{\pi^2} \right] \left(\frac{\lambda}{\pi^2} \right)^2, \end{aligned} \quad (1)$$

where $\mathcal{F}_{\text{ideal}} = -d_A \pi^2 T^4/6$ is the ideal or Stefan-Boltzmann limit of the free energy and $\mathcal{S}_{\text{ideal}} = 2d_A \pi^2 T^3/3$, with $d_A = N_c^2 - 1$ being the dimension of the adjoint representation and $\zeta(z)$ being the Riemann zeta function. The ratios of the free energy and entropy density to their corresponding ideal limit are the same owing to the fact that the 't Hooft coupling is temperature independent. Note, importantly that the weak-coupling expression (1) is valid for all N_c .

In the strong-coupling limit, the behavior of the $\text{SYM}_{4,4}$ free energy has been computed using the AdS/CFT correspondence. Most information is known about the large- N_c limit where one has [7]

$$\frac{\mathcal{F}}{\mathcal{F}_{\text{ideal}}} = \frac{\mathcal{S}}{\mathcal{S}_{\text{ideal}}} = \frac{3}{4} \left[1 + \frac{15}{8} \zeta(3) \lambda^{-3/2} + \mathcal{O}(\lambda^{-2}) \right]. \quad (2)$$

One issue that must be faced when using strict weak- or strong-coupling expansions is that they might have poor convergence as additional orders are included in the expansion or may not converge at all. This is a known issue with the weak-coupling expansion of QCD thermodynamics, in which case the series seems to converge only for $T \gtrsim 10^5$ GeV. This poor convergence of strict perturbation theory motivated research into methods for reorganizing the weak-coupling expansion in order to improve its convergence as one goes to higher loop order. In the context of QCD, the methods used have included the Φ -derivable method [38–41] and the hard-thermal-loop perturbation theory (HTLpt) reorganization [8,10,12].

Despite its appeal, a fundamental issue with the Φ -derivable method is that it is not manifestly gauge invariant, with gauge parameter dependence appearing at the same order in λ as the series truncation when evaluated off the stationary point and at twice the order in λ when

evaluated at the stationary point [9,42,43]. The HTLpt approach, on the contrary, is manifestly gauge invariant due to the fact that the HTL effective action used as the starting point is gauge invariant by construction. HTLpt has been used to improve the convergence of weak coupling calculations of the free energy in scalar field theories [44–46], QED [47], and QCD up to three-loop order at finite temperature and chemical potential [19–23,26,27]. Based on its success in QCD applications, in Ref. [48] we applied this method to $\text{SYM}_{4,4}$; however, in this prior work canonical dimensional regularization (DRG) [49–51] was used to regulate divergences generated during the calculation in the same manner as was done in QCD.

One issue with this prior work is that the use of canonical DRG breaks supersymmetry because in DRG the size of the bosonic representation depends on the dimensional regularization parameter ϵ . In this paper we address this issue by using a regularization scheme called regularization by dimensional reduction (RDR). The RDR method was introduced by Siegel [52] and is a modified version of dimensional regularization [53,54] which manifestly preserves gauge invariance, unitarity, and supersymmetry [55,56]. In Refs. [36,37] this method was used to compute the λ^2 and $\lambda^2 \log \lambda$ coefficients in Eq. (1). Herein we will compute the order λ , $\lambda^{3/2}$, and $\lambda^2 \log \lambda$ coefficients using two-loop HTLpt and demonstrate that these coefficients are scheme independent. We will additionally demonstrate that the order λ^2 coefficient is regularization-scheme dependent; however, this is somewhat expected, since this coefficient is beyond the strict perturbative accuracy of a two-loop calculation. Importantly, we find that the coefficient of $\lambda^2 \log \lambda$ is exactly the same as obtained in the prior two-loop DRG HTLpt calculation [48], resummation using the Arnold-Zhai method [36], and resummation using effective field theory methods [37]. This firmly establishes the existence of logarithms in the weak-coupling expansion of $\text{SYM}_{4,4}$ thermodynamics and provides confidence in the computed coefficient.

Note that since the high-order terms in the expansion of the free energy are unknown, it is not possible to determine if the finite temperature perturbative series for the free energy has a finite radius of convergence. We note, however, that even if the perturbative series has a zero radius of convergence (an asymptotic series), it is possible to apply variational perturbation theory methods such as HTLpt to improve the convergence of successive loop approximations. In cases where all orders expansions of quantities are known, e.g., the ground state energy of a zero temperature anharmonic oscillator [57,58], it has been shown that by using variational perturbation theory one can even self-consistently obtain the strong coupling limit coefficients from a divergent weak-coupling expansion [59,60].

In the case of $\text{SYM}_{4,4}$, our recent calculations through order λ^2 [36,37] suggest that the perturbative expansion of $\text{SYM}_{4,4}$ thermodynamics has a finite and potentially large

radius of convergence. The resummed results obtained in this paper show that HTLpt can be used to improve the convergence of successive approximations to the $\text{SYM}_{4,4}$ free energy. As will we demonstrate, the two-loop HTLpt resummed result, although having strict perturbative accuracy of order $\lambda^{3/2}$, reproduces the order λ^2 result to within 2% for $\lambda \lesssim 2$ (see Fig. 2 below).

Finally, we emphasize that the scheme dependence discussed herein is related to whether or not one uses a supersymmetry-preserving regularization scheme. This is a fundamental symmetry requirement and, hence, the RDR scheme is better suited to this problem. In the context of QED and QCD there exists a more general scheme dependence which stems from the choice of the method of regularization. The standard scheme for renormalizing QCD is the $\overline{\text{MS}}$ (modified minimal subtraction) scheme [61], which is related to the MS (minimal subtraction) scheme [62,63] through a rescaling of the MS scale by $(e^{\gamma_E}/4\pi)^\epsilon$ where γ_E is the Euler-Mascheroni constant. As a result of this relationship, one can connect quantities computed in the two schemes in a straightforward manner using the running coupling itself [61]. We note importantly, however, that physical observables such as scattering rates and the free energy are scheme independent [61,64,65]. In strict perturbation theory, renormalization scheme invariance of observables can be established order-by-order in the coupling; however, the parameters in the theory which are not directly observable, such as the running coupling constant, are in general scheme dependent. When computing observables the scheme-dependence of the parameters is compensated for by the scheme-dependence of the coefficients in the perturbative expansion thereby ensuring renormalization group invariance [61,64,65].

In $\text{SYM}_{4,4}$ an analogous scheme dependence does not occur because the theory is conformal and the coupling does not run. As a result, the perturbative coefficients are renormalization group invariants and hence, scheme independent in the QED/QCD sense. This is evidenced by Eq. (1) which is scale invariant through the perturbative accuracy determined. Finally, we note that HTLpt goes beyond strict perturbation theory through an all orders resummation in the soft sector. As a result, a residual scale dependence can remain in HTLpt when truncating at finite loop order; however, as one extends the HTLpt calculation to higher loop order, the scale dependence is systematically pushed to higher orders in the 't Hooft coupling, resulting in mathematically unique predictions for the fully determined perturbative coefficients.

The structure of our paper is as follows. We begin with a brief introduction to the basics of $\text{SYM}_{4,4}$ in Sec. II. In Sec. III, we present a summary of HTLpt applied to $\text{SYM}_{4,4}$. We list the terms which change in the high temperature expansion when going from DRG to RDR in Sec. IV. Based on these results, we present the complete expressions for the leading- (LO) and next-to-leading order

(NLO) thermodynamic potentials in the RDR scheme in Sec. V. In Sec. VI, we present our numerical results for the RDR HTLpt-resummed NLO $\text{SYM}_{4,4}$ scaled thermodynamic functions and compare to our previous results obtained using the DRG scheme. We also compare to strict perturbative expression for the scaled thermodynamic functions through order λ^2 which were obtained using the RDR scheme and to a generalized Padé approximant based on this result and the corresponding result in the large- N_c strong coupling limit. In Sec. VII we present our conclusions and an outlook for the future.

Notation: We use lower-case letters for Minkowski space four-vectors, e.g., p , and upper-case letters for Euclidean space four-vectors, e.g., P . We use the mostly minus convention for the metric.

II. THE BASICS OF THE $\text{SYM}_{4,4}$ THEORY

In $\text{SYM}_{4,4}$ all fields belong to the adjoint representation of the $SU(N_c)$ gauge group. The definition of gauge field is the same as QCD and A_μ can be expanded as $A_\mu = A_\mu^a t^a$, with real coefficients A_μ^a , and Hermitian color generators t^a in the adjoint representation which satisfy

$$[t^a, t^b] = if_{abc}t^c \quad \text{and} \quad \text{Tr}(t^a t^b) = \frac{1}{2}\delta^{ab}, \quad (3)$$

where $a, b = 1, \dots, N_c^2 - 1$ and the group structure constants f_{abc} are real and completely antisymmetric.

For the fermionic fields, the massless two-component Weyl fermions ψ in four dimensions can be converted into four-component Majorana fermions [66–70],

$$\psi \equiv \begin{pmatrix} \psi_\alpha \\ \bar{\psi}^{\dot{\alpha}} \end{pmatrix} \quad \text{and} \quad \bar{\psi} \equiv (\psi^\alpha \quad \bar{\psi}_{\dot{\alpha}}), \quad (4)$$

where $\alpha = 1, 2$ and the Weyl spinors satisfy $\bar{\psi}^{\dot{\alpha}} \equiv [\psi^\alpha]^\dagger$. The conjugate Majorana spinor $\bar{\psi}$ is not independent, but is related to ψ via the Majorana condition $\psi = C\bar{\psi}$, where $C = \begin{pmatrix} \epsilon^{\alpha\beta} & 0 \\ 0 & \epsilon^{\dot{\alpha}\dot{\beta}} \end{pmatrix}$ is the charge conjugation operator with $\epsilon_{02} = -\epsilon_{11} \equiv -1$. We will use latin indices $i, j = 1, 2, 3, 4$ to label the four Majorana fermions, with ψ_i denoting each bispinor. Since the fermions are in the adjoint representation, one can expand $\psi_i = \psi_i^a t^a$, where the coefficients ψ_i^a are four-component Grassmann-valued Majorana spinors.

In addition to the gauge field and Majorana spinors, there are six independent real scalar fields which are represented by a multiplet,

$$\Phi \equiv (X_1, Y_1, X_2, Y_2, X_3, Y_3), \quad (5)$$

where X_p and Y_q are Hermitian, with $p, q = 1, 2, 3$. X_p and Y_q denote scalar and pseudoscalar fields, respectively. We will use a capital latin index A to denote components of the

vector Φ . Therefore Φ_A , X_p , and Y_q can be expanded as $\Phi_A = \Phi_A^a t^a$, with $A = 1, \dots, 6$ or alternatively, $X_p = X_p^a t^a$ and $Y_q = Y_q^a t^a$.

The Minkowski-space Lagrangian density for $\text{SYM}_{4,4}$ can be expressed as

$$\begin{aligned} \mathcal{L}_{\text{SYM}_{4,4}} = & \text{Tr} \left[-\frac{1}{2} G_{\mu\nu}^2 + (D_\mu \Phi_A)^2 + i\bar{\psi}_i \not{D} \psi_i \right. \\ & \left. - \frac{1}{2} g^2 (i[\Phi_A, \Phi_B])^2 - ig\bar{\psi}_i [\alpha_{ij}^p X_p + i\beta_{ij}^q Y_q, \psi_j] \right] \\ & + \mathcal{L}_{\text{gf}} + \mathcal{L}_{\text{gh}} + \Delta\mathcal{L}_{\text{SYM}}, \end{aligned} \quad (6)$$

where $\mu, \nu = 0, 1, 2, 3$ and α^p and β^q are 4×4 matrices that satisfy

$$\{\alpha^p, \alpha^q\} = -2\delta^{pq}, \quad \{\beta^p, \beta^q\} = -2\delta^{pq}, \quad [\alpha^p, \beta^q] = 0. \quad (7)$$

The matrices α and β satisfy $\alpha_{ik}^p \alpha_{kj}^p = -3\delta_{ij}$ and $\beta_{ij}^q \beta_{ji}^q = -4\delta^{pq}$, with $\delta_{ii} = 4$ for the four Majorana fermions and $\delta^{pp} = 3$ for each set of three scalars.

To quantize the theory, gauge-fixing and ghost terms should be added to the Lagrangian density. In general covariant gauge, their forms are the same as in QCD,

$$\begin{aligned} \mathcal{L}_{\text{gf}}^{\text{SYM}_{4,4}} &= -\frac{1}{\xi} \text{Tr}[(\partial^\mu A_\mu)^2], \\ \mathcal{L}_{\text{gh}}^{\text{SYM}_{4,4}} &= -2\text{Tr}[\bar{\eta} \partial^\mu D_\mu \eta], \end{aligned} \quad (8)$$

with ξ being the gauge parameter.

III. HTLpt FOR $\text{SYM}_{4,4}$ THEORY

HTLpt provides a way to incorporate plasma effects into resummed perturbative calculations while maintaining explicit gauge invariance. In HTLpt the underlying theory is reorganized by adding and subtracting the HTL effective action to the vacuum action. The addition/subtraction of the HTLpt action generates effective propagators and vertices which are functions of energy and momentum. The HTLpt method has been applied to QCD to three-loop order in Refs. [8,10,12,16,17,19–29].

The HTLpt reorganization of $\text{SYM}_{4,4}$ can be obtained in the same manner as in QCD by introducing an expansion parameter δ , treating it as a formal expansion parameter, expanding around $\delta = 0$ to a fixed order, and then setting $\delta = 1$ in the end. The HTL reorganized Lagrangian density for $\text{SYM}_{4,4}$ can be written as

$$\mathcal{L}_{\text{SYM}_{4,4}}^{\text{shifted}} = (\mathcal{L}_{\text{SYM}_{4,4}} + \mathcal{L}_{\text{SYM}_{4,4}}^{\text{HTL}})|_{g \rightarrow \sqrt{\delta}g} + \Delta\mathcal{L}_{\text{SYM}_{4,4}}^{\text{HTL}}. \quad (9)$$

The HTL improvement term $\mathcal{L}_{\text{SYM}_{4,4}}^{\text{HTL}}$ is

$$\begin{aligned} \mathcal{L}_{\text{SYM}_{4,4}}^{\text{HTL}} = & -\frac{1}{2}(1-\delta)m_D^2 \text{Tr} \left(G_{\mu\alpha} \left\langle \frac{y^\alpha y^\beta}{(y \cdot D)^2} \right\rangle_{\hat{y}} G_{\beta}^\mu \right) \\ & + (1-\delta)im_q^2 \text{Tr} \left(\bar{\psi}_j \gamma^\mu \left\langle \frac{y^\mu}{y \cdot D} \right\rangle_{\hat{y}} \psi_j \right) \\ & - (1-\delta)M_D^2 \text{Tr}(\Phi_A^2), \end{aligned} \quad (10)$$

where $y^\mu = (1, \hat{y})$ is a lightlike four vector, $\langle \cdot \cdot \cdot \rangle_{\hat{y}}$ represents an average over the direction of \hat{y} defined in the Appendix A, the index $j \in \{1 \dots 4\}$ labels the four Majorana fermions, and the index $A \in \{1 \dots 6\}$ labels the six independent real-valued scalars. The parameters m_D and M_D are the electric screening masses for the gauge field and the adjoint scalar fields, respectively. The parameter m_q is the induced finite temperature quark mass. We note that, in general, the gluon mass in RDR is not equal to $-g_{\mu\nu} \Pi^{\mu\nu}$, where $\Pi^{\mu\nu}$ is the gluonic self energy and care must be taken due to this. This stems from the necessity of employing integration by parts during the calculation of the gluon self energy.

In the RDR scheme, all momentum-space integrals will be evaluated in $d = 4 - 2\epsilon$ dimensions while the size of the gauge field and fermionic field representations will be taken to be integer valued, and correspond to $D = 4$ dimensional fields. Since, as we will demonstrate, all ultraviolet divergences generated in the calculation of HTL-thermodynamics are canceled by the HTLpt counterterms independently of the value of the gluon, quark, and scalar mass parameters, we need to only consider the leading-order contributions in the momentum-space regulation parameter ϵ .

The HTLpt reorganization of QCD and $\text{SYM}_{4,4}$ generates new ultraviolet (UV) divergences compared to the vacuum Lagrangian. In QCD, these divergences can be eliminated using the counterterm Lagrangian $\Delta\mathcal{L}_{\text{QCD}}^{\text{HTL}}$, and the thermodynamic potential at the two-loop level can be renormalized by using a simple counterterm Lagrangian $\Delta\mathcal{L}_{\text{QCD}}^{\text{HTL}}$ which includes vacuum energy and mass counterterms [16,17]. Although not proven at arbitrary loop order, it has been explicitly demonstrated that one can renormalize the HTLpt thermodynamic potential through three-loop order using only vacuum, gluon thermal mass, quark thermal mass, and gauge coupling constant counterterms [22,27]. The same method can be used in $\text{SYM}_{4,4}$.

We find that in $\text{SYM}_{4,4}$ the vacuum counterterm $\Delta_0 \mathcal{E}_0$, which is the leading order counterterm in the δ expansion of the vacuum energy \mathcal{E}_0 , can be obtained by calculating the free energy to leading order in δ , and the next-to-leading-order contribution $\Delta_1 \mathcal{E}_0$ can be obtained by expanding $\Delta \mathcal{E}_0$ to linear order in δ . As a result, we find that in the RDR scheme the counterterm $\Delta \mathcal{E}_0$ has the form,

$$\begin{aligned} \Delta \mathcal{E}_0 = & \left(\frac{d_A}{128\pi^2\epsilon} + O(\lambda\delta) \right) (1-\delta)^2 m_D^4 \\ & + \left(\frac{3d_A}{32\pi^2\epsilon} + O(\lambda\delta) \right) (1-\delta)^2 M_D^4. \end{aligned} \quad (11)$$

Comparing to the DRG HTLpt result obtained in Ref. [48], one sees that Eq. (11) is precisely the same as obtained therein.

To calculate the NLO HTLpt-improved free energy one needs to expand the partition function to order δ . Correspondingly, to cancel the remaining UV divergences we need the counterterms $\Delta\mathcal{E}_0$, Δm_D^2 , Δm_q^2 , and ΔM_D^2 to order δ . In order to remove all UV divergences which appear at two-loop level, the mass counterterms required are

$$\begin{aligned}\Delta m_D^2 &= \left(\frac{1}{16\pi^2\epsilon} \lambda\delta + O(\lambda^2\delta^2) \right) (1-\delta)m_D^2, \\ \Delta M_D^2 &= \left(\frac{3}{8\pi^2\epsilon} \lambda\delta + O(\lambda^2\delta^2) \right) (1-\delta)M_D^2, \\ \Delta m_q^2 &= \left(-\frac{1}{\pi^2\epsilon} \lambda\delta + O(\lambda^2\delta^2) \right) (1-\delta)m_q^2.\end{aligned}\quad (12)$$

Once again we find that the mass counterterms are precisely the same as the ones necessary to remove the HTLpt divergences in DRG HTLpt [48].

To calculate HTLpt-improved physical observables in $\text{SYM}_{4,4}$ we use the same method as in QCD, namely expanding the path-integral in powers of δ , truncating at some specified order, and then setting $\delta = 1$. The results for physical observables will depend on m_D , M_D , and m_q which are functions of T and λ . These parameters are fixed in HTLpt by minimizing the free energy. If we use $\Omega_N^{\text{RDR}}(T, \lambda, m_D, M_D, m_q, \delta)$ to represent the thermodynamic potential expanded to N -th order in δ , then the corresponding variational prescription is

$$\begin{aligned}\frac{\partial}{\partial m_D} \Omega_N^{\text{RDR}}(T, \lambda, m_D, M_D, m_q, \delta = 1) &= 0, \\ \frac{\partial}{\partial M_D} \Omega_N^{\text{RDR}}(T, \lambda, m_D, M_D, m_q, \delta = 1) &= 0, \\ \frac{\partial}{\partial m_q} \Omega_N^{\text{RDR}}(T, \lambda, m_D, M_D, m_q, \delta = 1) &= 0.\end{aligned}\quad (13)$$

These three equations are called the *gap equations*. The free energy can be obtained by evaluating the thermodynamic potential at the solution to the gap equations, and other thermodynamic functions can be obtained from the free energy and its derivatives with respect to T .

In the following section, we calculate the thermodynamic potential through order $\lambda^{5/2}$, which can be expressed as an expansion in powers of m_D/T , m_q/T , and M_D/T . Instead of repeating all results from our DRG calculation, we list all terms which change when going from DRG to RDR. As mentioned above, at order δ , all divergences in the two-loop thermodynamic potential can be removed by the HTLpt vacuum and mass counterterms which are scheme independent.

IV. HIGH-TEMPERATURE EXPANSION USING THE RDR SCHEME

In this section, we list only the contributions which change when going from the DRG to RDR scheme. Since the Feynman rules and diagrams needed are the same as in Ref. [48], the high-temperature forms are the same as in this reference up to the dimension of the gluon tensor and metric tensor. The labels on each Feynman diagram contribution below correspond to the diagrams shown in Ref. [48].

A. One-loop sum-integrals in the RDR scheme

Based on the above knowledge, at one-loop order, only the hard contribution from the gluonic one-loop free energy and two-loop HTL counterterm are modified in the RDR scheme. The remaining contributions come from fermions and scalars and remain unchanged compared to the DRG HTLpt result.

1. RDR modified gluon hard contributions

The form of the hard contribution to the one-loop gluon free energy expanded to second order in m_D^2 has been given in [16] and can be written in the RDR scheme as

$$\begin{aligned}\mathcal{F}_g^{(h),\text{RDR}} &= \frac{D-2}{2} b_0 + \frac{1}{2} m_D^2 b_1 - \frac{1}{4(D-2)} m_D^4 b_2 \\ &\quad - \frac{1}{4(D-2)} m_D^4 \sum_p \left[-2 \frac{1}{p^2 P^2} - 2(D-1) \frac{1}{p^4} \mathcal{T}_p \right. \\ &\quad \left. + 2 \frac{1}{p^2 P^2} \mathcal{T}_p + (D-1) \frac{1}{p^4} (\mathcal{T}_p)^2 \right],\end{aligned}\quad (14)$$

where \mathcal{T}_p is given in Eq. (A14), which enters into the HTL gluon self-energy, and

$$b_0 \equiv \sum_p \log P^2 = -\frac{\pi^2}{45} T^4, \quad (15)$$

$$b_n \equiv \sum_p \frac{1}{P^{2n}}, \quad n \geq 1. \quad (16)$$

Setting $D = 4$, using Eq. (15), and the formulas in Appendix B, (14) reduces to

$$\begin{aligned}\mathcal{F}_g^{(h),\text{RDR}} &= -\frac{\pi^2}{45} T^4 + \frac{1}{24} \left[1 + \left(2 + 2 \frac{\zeta'(-1)}{\zeta(-1)} \right) \epsilon \right] \\ &\quad \times \left(\frac{\mu}{4\pi T} \right)^{2\epsilon} m_D^2 T^2 - \frac{1}{128\pi^2} \left(\frac{1}{\epsilon} + 2\gamma + \frac{2\pi^2}{3} \right. \\ &\quad \left. - \frac{16}{3} - \frac{8 \log 2}{3} \right) \left(\frac{\mu}{4\pi T} \right)^{2\epsilon} m_D^4.\end{aligned}\quad (17)$$

The form of the hard contribution to the two-loop gluon HTL counterterm has been given in [16] and can be expressed as

$$\begin{aligned}\mathcal{F}_{gct}^{(h),\text{RDR}} &= -\frac{1}{2}m_D^2 b_1 + \frac{1}{2(D-2)}m_D^4 b_2 \\ &+ \frac{1}{2(D-2)}m_D^4 \sum_P \left[-2\frac{1}{p^2 P^2} - 2(D-1)\frac{1}{p^4} T_P \right. \\ &\left. + 2\frac{1}{p^2 P^2} T_P + (D-1)\frac{1}{p^4} (T_P)^2 \right].\end{aligned}\quad (18)$$

Setting $D = 4$, using Eq. (15), and the formulas in Appendix B, (18) reduces to

$$\begin{aligned}\mathcal{F}_{gct}^{(h),\text{RDR}} &= -\frac{1}{24}m_D^2 T^2 + \frac{1}{64\pi^2} \left[\frac{1}{\epsilon} + 2\gamma + \frac{2\pi^2}{3} \right. \\ &\left. - \frac{16}{3} - \frac{8 \log 2}{3} \right] \left(\frac{\mu}{4\pi T} \right)^{2\epsilon} m_D^4.\end{aligned}\quad (19)$$

We find, as can be expected on general grounds, that the only difference between the result of the one-loop

gluonic contributions in the RDR scheme and the DRG scheme is the finite contribution which is proportional to m_D^4 .

B. Two-loop sum-integrals in the RDR scheme

Considering the two-loop contributions in the RDR scheme, the soft-soft (ss) contribution from all diagrams and the $\mathcal{F}_{3qs}^{(hh)}$ contribution are unchanged. All other contributions are modified due to the dimension of the gluon tensor and metric tensor changing from $4 - 2\epsilon$ to 4.

1. Contributions from the (hh) region

The form of the (hh) contributions to the two-loop gluonic free energy expanded to first order in m_D^2 has been given in [16], and can be written in the RDR scheme as

$$\begin{aligned}\mathcal{F}_{3g+4g+gh}^{(hh),\text{RDR}} &= \frac{1}{4}(D-2)^2 b_1^2 - (D-2)\frac{1}{2}m_D^2 b_1 b_2 + \frac{1}{4}m_D^2 \sum_{PQ} \left\{ 2(D-3)\frac{1}{P^2 Q^2 q^2} + 2\frac{1}{P^2 Q^2 R^2} \right. \\ &+ (D+1)\frac{1}{P^2 Q^2 r^2} - 2(D-1)\frac{P \cdot Q}{P^2 Q^2 r^4} - 4(D-1)\frac{q^2}{P^2 Q^2 r^4} + 4\frac{q^2}{P^2 Q^2 R^2 r^2} - 2(D-2)\frac{1}{P^2 Q^2 q^2} T_Q \\ &\left. - D\frac{1}{P^2 Q^2 r^2} T_R + 4(D-1)\frac{q^2}{P^2 Q^2 r^4} T_R + 2(D-1)\frac{P \cdot Q}{P^2 Q^2 r^4} T_R \right\}.\end{aligned}\quad (20)$$

Setting $D = 4$, using Eq. (15), and the formulas in Appendix B, (20) reduces to

$$\mathcal{F}_{3g+4g+gh}^{(hh),\text{RDR}} = \frac{1}{144} T^4 - \frac{29}{4608\pi^2} \left(\frac{1}{\epsilon} + 5.751206124 \right) \left(\frac{\mu}{4\pi T} \right)^{4\epsilon} m_D^2 T^2.\quad (21)$$

The form of the (hh) contribution to \mathcal{F}_{3qg} and \mathcal{F}_{4qg} expanded to first order in m_D^2 can be obtained from Ref. [17], and in the RDR scheme become

$$\begin{aligned}\mathcal{F}_{3qg+4qg}^{(hh),\text{RDR}} &= 2(D-2)[f_1^2 - 2b_1 f_1] + 4m_D^2 \left\{ b_2 f_1 + \sum_{P\{Q\}} \left[\frac{1}{p^2 P^2 Q^2} T_P - \frac{D-3}{D-2} \frac{1}{p^2 P^2 Q^2} \right] \right\} \\ &+ 2m_D^2 \sum_{\{PQ\}} \left[\frac{D}{D-2} \frac{1}{P^2 Q^2 r^2} - \frac{4(D-1)}{D-2} \frac{q^2}{P^2 Q^2 r^4} - \frac{2(D-1)}{D-2} \frac{P \cdot Q}{P^2 Q^2 r^4} \right] T_R \\ &+ 2m_D^2 \sum_{\{PQ\}} \left[\frac{4-D}{D-2} \frac{1}{P^2 Q^2 R^2} + \frac{2(D-1)}{D-2} \frac{P \cdot Q}{P^2 Q^2 r^4} - \frac{D+1}{D-2} \frac{1}{P^2 Q^2 r^2} + \frac{4(D-1)}{D-2} \frac{q^2}{P^2 Q^2 r^4} - \frac{4}{D-2} \frac{q^2}{P^2 Q^2 R^2 r^2} \right] \\ &+ 4m_q^2 (D-2) \sum_{\{PQ\}} \left[\frac{1}{P^2 Q^2 Q_0^2} + \frac{p^2 - r^2}{P^2 q^2 Q_0^2 R^2} \right] T_Q + 4m_q^2 (D-2) \left[2b_1 f_2 - \sum_{P\{Q\}} \frac{1}{P^2 Q^2 Q_0^2} T_Q \right] \\ &+ 4m_q^2 (D-2) \left\{ -2f_1 f_2 + \sum_{\{PQ\}} \left[\frac{D-6}{D-2} \frac{1}{P^2 Q^2 R^2} + \frac{r^2 - p^2}{P^2 Q^2 R^2 q^2} \right] \right\},\end{aligned}\quad (22)$$

where f_n is defined as

$$f_n \equiv \sum_{\{P\}} \frac{1}{P^{2n}} = (2^{2n+1-d} - 1) b_n, \quad n \geq 1.\quad (23)$$

Setting $D = 4$, using Eqs. (15) and (23), and formulas in Appendix B, (22) reduces to

$$\begin{aligned} \mathcal{F}_{3gq+4qg}^{(hh),\text{RDR}} &= \frac{5}{144} T^4 - \frac{7}{1152\pi^2} \left[\frac{1}{\epsilon} + 0.1415352337 \right] \\ &\times \left(\frac{\mu}{4\pi T} \right)^{4\epsilon} m_D^2 T^2 + \frac{1}{16\pi^2} \left[\frac{1}{\epsilon} + 9.96751112 \right] \\ &\times \left(\frac{\mu}{4\pi T} \right)^{4\epsilon} m_q^2 T^2. \end{aligned} \quad (24)$$

The form of the (hh) contributions to \mathcal{F}_{4s} , \mathcal{F}_{3gs} and \mathcal{F}_{4gs} are

$$\begin{aligned} \mathcal{F}_{4s+3gs+4gs}^{(hh),\text{RDR}} &= 3(D+1)b_1^2 - 3(4+D)M_D^2 b_1 b_2 + M_D^2 \\ &\times \int_{P,Q} \frac{6}{P^2 Q^2 R^2} - 3m_D^2 b_1 b_2 + m_D^2 \frac{3(D-3)}{D-2} b_1 \int_P \frac{1}{p^2 P^2} \\ &+ \frac{m_D^2}{D-2} \int_{P,Q} \left\{ \frac{3(1+D)}{2p^2 Q^2 R^2} - \frac{3}{P^2 Q^2 R^2} - \frac{6(D-1)q^2}{p^4 Q^2 R^2} \right. \\ &+ \frac{6q^2}{p^2 P^2 Q^2 R^2} + \frac{3(D-1)(Q \cdot R)}{p^4 Q^2 R^2} + \left. \left[\frac{3(2-D)}{p^2 P^2 Q^2} \right. \right. \\ &\left. \left. - \frac{3D}{2p^2 Q^2 R^2} + \frac{6(D-1)q^2}{p^4 Q^2 R^2} - \frac{3(D-1)(Q \cdot R)}{p^4 Q^2 R^2} \right] T_P \right\}. \end{aligned} \quad (25)$$

Setting $D = 4$, using Eq. (15), and the formulas in Appendix B, (25) reduces to

$$\begin{aligned} \mathcal{F}_{4s+3gs+4gs}^{(hh),\text{RDR}} &= \frac{5}{48} T^4 - \frac{1}{8\pi^2} \left(\frac{1}{\epsilon} + 2\gamma + 5.97010745 \right) \\ &\times \left(\frac{\mu}{4\pi T} \right)^{4\epsilon} M_D^2 T^2 - \frac{29}{1536\pi^2} \\ &\times \left(\frac{1}{\epsilon} + 5.751206124 \right) \left(\frac{\mu}{4\pi T} \right)^{4\epsilon} m_D^2 T^2. \end{aligned} \quad (26)$$

2. Contributions from the (hs) region

The form of the (hs) contribution to the two-loop gluon free energy expanded to first order in m_D^2 was given in [16], and in the RDR scheme can be written as

$$\begin{aligned} \mathcal{F}_{3g+4g+gh}^{(hs),\text{RDR}} &= \frac{T}{2} \int_{\mathbf{p}} \frac{1}{p^2 + m_D^2} \left\{ -(D-2)b_1 + 2(D-2) \right. \\ &\times \int_Q \frac{q^2}{Q^4} \left. \right\} + m_D^2 T \int_{\mathbf{p}} \frac{1}{p^2 + m_D^2} \left\{ -(D-5)b_2 \right. \\ &+ \int_Q \left[\frac{(D-2)(D+1)q^2}{D-1} \frac{1}{Q^6} - \frac{4(D-2)q^4}{D-1} \frac{1}{Q^8} \right] \left. \right\}, \end{aligned} \quad (27)$$

where

$$\int_{\mathbf{p}} \frac{1}{p^2 + m^2} = -\frac{m}{4\pi} \left(\frac{\mu}{2m} \right)^{2\epsilon} [1 + 2\epsilon]. \quad (28)$$

Setting $D = 4$, using Eqs. (15) and (28), and the formulas in Appendix B, (27) reduces to

$$\begin{aligned} \mathcal{F}_{3g+4g+gh}^{(hs),\text{RDR}} &= -\frac{1}{24\pi} m_D T^3 - \frac{11}{384\pi^3} \left(\frac{1}{\epsilon} + 2\gamma + \frac{68}{33} \right) \\ &\times \left(\frac{\mu}{4\pi T} \right)^{2\epsilon} \times \left(\frac{\mu}{2m_D} \right)^{2\epsilon} m_D^3 T. \end{aligned} \quad (29)$$

The form of the (hs) contribution to \mathcal{F}_{3qg} and \mathcal{F}_{4qg} expanded to first order in m_D^2 can be obtained from Ref. [17], and in the RDR scheme can be expressed as

$$\begin{aligned} \mathcal{F}_{3qg+4qg}^{(hs),\text{RDR}} &= T \int_{\mathbf{p}} \frac{1}{p^2 + m_D^2} \left[4f_1 - \int_{\{Q\}} \frac{8q^2}{Q^4} \right] \\ &+ 4m_D^2 T \int_{\mathbf{p}} \frac{1}{p^2 + m_D^2} \left\{ f_2 \right. \\ &+ \int_{\{Q\}} \left[-\frac{2(2+D)q^2}{D-1} \frac{1}{Q^6} + \frac{8}{D-1} \frac{q^4}{Q^8} \right] \left. \right\} \\ &- 8m_q^2 T \int_{\mathbf{p}} \frac{1}{p^2 + m_D^2} \left[3f_2 - \int_{\{Q\}} \frac{4q^2}{Q^6} \right]. \end{aligned} \quad (30)$$

Setting $D = 4$, using Eqs. (15), (23), and (28) together with the formulas in Appendix B, (30) reduces to

$$\begin{aligned} \mathcal{F}_{3qg+4qg}^{(hs),\text{RDR}} &= -\frac{1}{12\pi} m_D T^3 + \frac{1}{4\pi^3} m_D m_q^2 T \\ &+ \frac{1}{48\pi^3} \left(\frac{1}{\epsilon} + 2\gamma + \frac{4}{3} + 4 \log 2 \right) \\ &\times \left(\frac{\mu}{4\pi T} \right)^{2\epsilon} \left(\frac{\mu}{2m_D} \right)^{2\epsilon} m_D^3 T. \end{aligned} \quad (31)$$

The (hs) contribution to \mathcal{F}_{4s} , \mathcal{F}_{3gs} , and \mathcal{F}_{4gs} were presented in [48] and in the RDR scheme can be expressed as

$$\begin{aligned} \mathcal{F}_{4s+3gs+4gs}^{(hs),\text{RDR}} &= T \int_{\mathbf{p}} \frac{1}{p^2 + M_D^2} \left[3(D+4)b_1 - 3M_D^2 b_2 \right. \\ &\left. - 3m_D^2 b_2 - M_D^2 \int_Q \frac{12q^2}{(D-1)Q^6} \right] \\ &+ T \int_{\mathbf{p}} \frac{1}{p^2 + m_D^2} \times \left\{ -3b_1 + 9M_D^2 b_2 - 6m_D^2 b_2 \right. \\ &+ \int_Q \left[\frac{6q^2}{Q^4} - M_D^2 \frac{12q^2}{Q^6} \right. \\ &\left. \left. + m_D^2 \left(6 \frac{D+3}{D-1} \frac{q^2}{Q^6} - \frac{24q^4}{(D-1)Q^8} \right) \right] \right\}. \end{aligned} \quad (32)$$

Setting $D = 4$, using Eq. (15), and the formulas in Appendix B, (32) reduces to

$$\begin{aligned} \mathcal{F}_{4s+3gs+4gs}^{(hs),\text{RDR}} &= -T^3 \left(\frac{m_D}{8\pi} + \frac{M_D}{2\pi} \right) - \frac{3}{32\pi^3} M_D^2 m_D T \\ &+ \frac{3}{64\pi^3} \left(\frac{1}{\epsilon} + 2 + 2\gamma \right) \left(\frac{\mu}{4\pi T} \right)^{2\epsilon} \left(\frac{\mu}{2M_D} \right)^{2\epsilon} M_D m_D^2 T \\ &+ \frac{3}{32\pi^3} \left(\frac{1}{\epsilon} + \frac{5}{3} + 2\gamma \right) \left(\frac{\mu}{4\pi T} \right)^{2\epsilon} \left(\frac{\mu}{2M_D} \right)^{2\epsilon} M_D^3 T \\ &+ \frac{1}{128\pi^3} \left(\frac{1}{\epsilon} + \frac{16}{3} + 2\gamma \right) \left(\frac{\mu}{4\pi T} \right)^{2\epsilon} \left(\frac{\mu}{2m_D} \right)^{2\epsilon} m_D^3 T. \quad (33) \end{aligned}$$

Finally, the (hs) contribution to \mathcal{F}_{3qs} was first presented in [48] and in the RDR scheme is

$$\begin{aligned} \mathcal{F}_{3qs}^{(hs),\text{RDR}} &= 24T \int_{\mathbf{p}} \frac{1}{p^2 + M_D^2} \left[-f_1 - M_D^2 f_2 \right. \\ &\quad \left. + 2m_q^2 f_2 + M_D^2 \sum_{\{Q\}} \frac{2q^2}{(D-1)Q^6} \right]. \quad (34) \end{aligned}$$

Setting $D = 4$, using Eqs. (15), (23), and (28) together with the formulas in Appendix B, (34) reduces to

$$\begin{aligned} \mathcal{F}_{3qs}^{(hs),\text{RDR}} &= -\frac{1}{4\pi} M_D T^3 + \frac{3}{16\pi^3} \left(\frac{1}{\epsilon} + \frac{8}{3} + 2\gamma + 4 \log 2 \right) \\ &\times \left(\frac{\mu}{4\pi T} \right)^{2\epsilon} \left(\frac{\mu}{2M_D} \right)^{2\epsilon} M_D^3 T - \frac{3}{4\pi^3} \left(\frac{1}{\epsilon} + 2 + 2\gamma \right. \\ &\quad \left. + 4 \log 2 \right) \left(\frac{\mu}{4\pi T} \right)^{2\epsilon} \left(\frac{\mu}{2M_D} \right)^{2\epsilon} M_D m_q^2 T. \quad (35) \end{aligned}$$

V. NLO HTL THERMODYNAMIC POTENTIAL IN THE RDR SCHEME

In this section, we will combine all contributions and counterterms to obtain the LO and NLO HTLpt-resummed SYM_{4,4} thermodynamic potential $\Omega^{\text{RDR}}(T, \lambda, m_D, M_D, m_q, \delta = 1)$. In the following subsections, we list the various terms contributing and compare them to the corresponding results obtained in the DRG scheme.

A. Leading order

By combining Eq. (17) and contributions which are the same as in DRG scheme from Ref. [48], our final result for the one-loop free energy is

$$\begin{aligned} \Omega_{1\text{-loop}}^{\text{RDR}} &= \mathcal{F}_{\text{ideal}} \left\{ 1 - \hat{m}_D^2 + 4\hat{m}_D^3 - 6\hat{M}_D^2 + 24\hat{M}_D^3 \right. \\ &\quad \left. - 8\hat{m}_q^2 + 16\hat{m}_q^4(6 - \pi^2) + \frac{3}{4}\hat{m}_D^4 \left[\frac{1}{\epsilon} + 2\gamma + \frac{2\pi^2}{3} - \frac{16}{3} \right. \right. \\ &\quad \left. \left. + 2 \log \frac{\hat{\mu}}{2} - \frac{8 \log 2}{3} \right] + 9\hat{M}_D^4 \left[\frac{1}{\epsilon} + 2\gamma + 2 \log \frac{\hat{\mu}}{2} \right] \right\}, \quad (36) \end{aligned}$$

where \hat{m}_D , \hat{M}_D , \hat{m}_q and $\hat{\mu}$ are dimensionless variables, which are defined as

$$\begin{aligned} \hat{m}_D &= \frac{m_D}{2\pi T}, & \hat{M}_D &= \frac{M_D}{2\pi T}, \\ \hat{m}_q &= \frac{m_q}{2\pi T}, & \hat{\mu} &= \frac{\mu}{2\pi T}. \end{aligned} \quad (37)$$

Comparing to the one-loop free energy $\Omega_{1\text{-loop}}$ obtained in the DRG scheme, the only difference are the finite contributions which are proportional to m_D^4 . Since the RDR divergences are the same as in the DRG scheme, the corresponding leading order vacuum energy counterterm $\Delta_0 \mathcal{E}_0$ is also the same. After adding $\Delta_0 \mathcal{E}_0$ to (36), our final result for the LO renormalized thermodynamic potential in the RDR scheme is

$$\begin{aligned} \frac{\Omega_{\text{LO}}^{\text{RDR}}}{\mathcal{F}_{\text{ideal}}} &= 1 - \hat{m}_D^2 + 4\hat{m}_D^3 - 6\hat{M}_D^2 + 24\hat{M}_D^3 - 8\hat{m}_q^2 \\ &+ 16\hat{m}_q^4(6 - \pi^2) + \frac{3}{4}\hat{m}_D^4 \left[-\frac{16}{3} - \frac{8 \log 2}{3} + 2\gamma \right. \\ &\quad \left. + \frac{2\pi^2}{3} + 2 \log \frac{\hat{\mu}}{2} \right] + 18\hat{M}_D^4 \left[\gamma + \log \frac{\hat{\mu}}{2} \right]. \quad (38) \end{aligned}$$

B. Next-to-leading order

By combining Eqs. (20), (22), (26), (27), (30), (33), (35), and contributions which are the same as in DRG scheme from Ref. [48], and multiplying by λd_A , we obtain the final result for the two-loop HTLpt thermodynamic potential,

$$\begin{aligned} \frac{\Omega_{2\text{-loop}}^{\text{RDR}}}{\mathcal{F}_{\text{ideal}}} &= \frac{\lambda}{\pi^2} \left\{ -\frac{3}{2} + 3\hat{m}_D + 9\hat{M}_D - \frac{9}{2}\hat{M}_D\hat{m}_D + \frac{9}{2}\hat{m}_D\hat{M}_D^2 - 12\hat{m}_D\hat{m}_q^2 + \frac{3}{8}\hat{m}_D^2 \left[\frac{1}{\epsilon} + 4 \log \hat{m}_D \right. \right. \\ &\quad \left. \left. + 4 \log \frac{\hat{\mu}}{2} + 6.32087357 \right] + \frac{9}{4}\hat{M}_D^2 \left[\frac{1}{\epsilon} + 4 \log \hat{M}_D + 4 \log \frac{\hat{\mu}}{2} + 5.32488132 \right] - \hat{m}_D^3 \left[\frac{1}{2} + 4 \log 2 \right] \right. \\ &\quad \left. - 6\hat{m}_q^2 \left[\frac{1}{\epsilon} + 4 \log \frac{\hat{\mu}}{2} + 9.967511121 \right] - \hat{M}_D^3 \left(36 \log 2 + \frac{9}{2} \right) + 144 \log 2 \hat{M}_D \hat{m}_q^2 \right. \\ &\quad \left. + \left[-\frac{27}{2}\hat{M}_D^3 - \frac{9}{4}\hat{M}_D\hat{m}_D^2 + 36\hat{M}_D\hat{m}_q^2 \right] \left[2 + \frac{1}{\epsilon} + 2\gamma - 2 \log \hat{M}_D + 4 \log \frac{\hat{\mu}}{2} \right] \right\}. \quad (39) \end{aligned}$$

Comparing to the two-loop DRG result $\Omega_{2\text{-loop}}$, we find that there are differences in the finite contributions proportional to m_D^2 , M_D^2 , m_D^3 , m_q^2 and M_D^3 .

The NLO RDR HTLpt counterterm contribution is obtained from the sum of Eqs. (18) and contributions which are the same as in DRG scheme from Ref. [48], giving

$$\begin{aligned} \frac{\Omega_{\text{HTL}}^{\text{RDR}}}{\mathcal{F}_{\text{ideal}}} &= \hat{m}_D^2 - 6\hat{m}_D^3 + 6\hat{M}_D^2 - 36\hat{M}_D^3 + 8\hat{m}_q^2 \\ &+ 32\hat{m}_q^4(\pi^2 - 6) - \frac{3}{2}\hat{m}_D^4 \left[\frac{1}{\epsilon} + 2\gamma + 2\log\frac{\hat{\mu}}{2} + \frac{2\pi^2}{3} \right. \\ &\left. - \frac{16}{3} - \frac{8\log 2}{3} \right] - 18\hat{M}_D^4 \left[\frac{1}{\epsilon} + 2\gamma + 2\log\frac{\hat{\mu}}{2} \right]. \end{aligned} \quad (40)$$

$$\begin{aligned} \frac{\Omega_{\text{NLO}}^{\text{RDR}}}{\mathcal{F}_{\text{ideal}}} &= 1 - 2\hat{m}_D^3 - 12\hat{M}_D^3 + 16\hat{m}_q^4(\pi^2 - 6) - 18\hat{M}_D^4 \left(\gamma + \log\frac{\hat{\mu}}{2} \right) - \frac{3}{2}\hat{m}_D^4 \left(\gamma + \frac{\pi^2}{3} + \log\frac{\hat{\mu}}{2} - \frac{8}{3} - \frac{4\log 2}{3} \right) \\ &+ \frac{\lambda}{\pi^2} \left[-\frac{3}{2} + 3\hat{m}_D + 9\hat{M}_D - \frac{9}{2}\hat{m}_D\hat{M}_D + \frac{9}{2}\hat{m}_D\hat{M}_D^2 - 12\hat{m}_D\hat{m}_q^2 - 12\hat{m}_q^2 \left(1.99870184 + \log\frac{\hat{\mu}}{2} \right) \right. \\ &+ \frac{3}{4}\hat{m}_D^2 \left(0.1753830597 + 2\log\hat{m}_D + \log\frac{\hat{\mu}}{2} \right) - \hat{m}_D^3 \left(\frac{1}{2} + 4\log 2 \right) + \frac{9}{2}\hat{M}_D^2 \left(-0.3226130662 + 2\log\hat{M}_D + \log\frac{\hat{\mu}}{2} \right) \\ &\left. - \frac{9}{2}\hat{M}_D\hat{m}_D^2 \left(\gamma + \log\frac{\hat{\mu}}{2} \right) + 72\hat{M}_D\hat{m}_q^2 \left(\gamma + 2\log 2 + \log\frac{\hat{\mu}}{2} \right) - 9\hat{M}_D^3 \left(\frac{1}{2} + 3\gamma + 4\log 2 + 3\log\frac{\hat{\mu}}{2} \right) \right]. \end{aligned} \quad (41)$$

Note that the final expression is free from singularities and valid for all N_c . Comparing to the result obtained using the DRG scheme in Ref. [48], we find differences in terms without logarithms, which are proportional to m_D^4 , λm_q^2 , λm_D^2 , λM_D^2 , λm_D^3 and λM_D^3 . These terms all contribute to the coefficient of λ^2 in the strict perturbative limit.

C. The strict perturbative limit

We next consider the strict perturbative limit through order λ^2 . To obtain this limit we evaluate the NLO HTLpt thermodynamic potential with LO perturbative gluon, scalar, and quark masses. Expressed numerically, the NLO HTLpt result in the DRG scheme obtained in Ref. [48] is

$$\begin{aligned} \frac{\Omega_{\text{NLO}}^{\text{DRG}}}{\mathcal{F}_{\text{ideal}}} \Big|_{\substack{\hat{m}_q = \hat{m}_{q,\text{LO}} \\ \hat{m}_D = \hat{m}_{D,\text{LO}} \\ \hat{M}_D = \hat{M}_{D,\text{LO}}}} &= 1 - 0.151982\lambda + 0.142365\lambda^{3/2} \\ &- 0.0923192\lambda^2 + 0.015399\lambda^2 \log\frac{\lambda}{\hat{\mu}}, \end{aligned} \quad (42)$$

where $\hat{m}_{q,\text{LO}}$, $\hat{m}_{D,\text{LO}}$, and $\hat{M}_{D,\text{LO}}$ are taken to be given by their leading-order weak-coupling limits given in Eq. (A1). The corresponding RDR HTLpt result obtained herein is

Comparing to the DRG scheme result for Ω_{HTL} , the only difference is the finite contribution proportional to m_D^4 . We find that the form of $\Delta_1 \mathcal{E}_0$ is the same as in the DRG scheme. Since the divergent terms in Eq. (39) are the same as the ones in the DRG scheme, we find the same result for $\Delta \Omega_{\text{NLO}}^{\text{RDR}}$ as in the DRG scheme.

By adding the one-loop (38), and two-loop (39) HTLpt thermodynamic potentials, the HTLpt gluon and quark counterterms, and the HTLpt vacuum and mass renormalizations, we obtain the final expression for the NLO HTL thermodynamic potential in $\text{SYM}_{4,4}$ theory in the RDR scheme,

$$\begin{aligned} \frac{\Omega_{\text{NLO}}^{\text{RDR}}}{\mathcal{F}_{\text{ideal}}} \Big|_{\substack{\hat{m}_q = \hat{m}_{q,\text{LO}} \\ \hat{m}_D = \hat{m}_{D,\text{LO}} \\ \hat{M}_D = \hat{M}_{D,\text{LO}}}} &= 1 - 0.151982\lambda + 0.142365\lambda^{3/2} \\ &- 0.0912209\lambda^2 + 0.015399\lambda^2 \log\frac{\lambda}{\hat{\mu}}. \end{aligned} \quad (43)$$

We find the same dependence on the renormalization scale $\hat{\mu}$ and all terms are same except the term proportional to λ^2 without logarithms. We note that the coefficient of $\lambda^2 \log \lambda$ is the same using both schemes, showing that it is scheme independent.

As further a comparison, the perturbative free energy computed to three-loop order, keeping all terms through order λ^2 was obtained in Refs. [36,37]. Expressed numerically the full result is

$$\begin{aligned} \frac{F_{3\text{-loop}}^{\text{resum}}}{\mathcal{F}_{\text{ideal}}} &= 1 - 0.151982\lambda + 0.142365\lambda^{3/2} \\ &- 0.0613173\lambda^2 + 0.015399\lambda^2 \log \lambda. \end{aligned} \quad (44)$$

Comparing Eqs. (42) and (43) to (44), we find all terms are the same except the terms proportional to λ^2 . This is expected since both the RDR and DRG scheme HTLpt calculations were two-loop calculations and hence cannot reproduce the full λ^2 coefficient. At two-loop order one could consider fixing $\hat{\mu}$ as to reproduce the full order λ^2

coefficient. This occurs when $\hat{\mu} \simeq 0.133554$ and $\hat{\mu} \simeq 0.143428$, in the DRG and RDR schemes, respectively.

D. Gap equations

To go beyond strict perturbation theory we need to fix the mass parameters in a nonperturbative manner. Using the NLO HTLpt thermodynamic potential, the gluon, scalar, and quark masses can be fixed using the variational method described previously. The gluon, scalar, and quark mass parameters m_D , M_D , and m_q can be determined by requiring the derivative of $\Omega_{\text{NLO}}^{\text{RDR}}$ with respect to each parameter is zero,

$$\begin{aligned} \frac{\partial}{\partial m_q} \Omega_{\text{NLO}}^{\text{RDR}}(T, \lambda, m_D, M_D, m_q, \delta = 1) &= 0, \\ \frac{\partial}{\partial m_D} \Omega_{\text{NLO}}^{\text{RDR}}(T, \lambda, m_D, M_D, m_q, \delta = 1) &= 0, \\ \frac{\partial}{\partial M_D} \Omega_{\text{NLO}}^{\text{RDR}}(T, \lambda, m_D, M_D, m_q, \delta = 1) &= 0. \end{aligned} \quad (45)$$

The first equation in Eq. (45) gives

$$\begin{aligned} \hat{m}_q^2(\pi^2 - 6) &= \frac{\lambda}{4\pi^2} \left[\frac{3}{2} \hat{m}_D + \frac{3}{2} \left(1.998701836 + \log \frac{\hat{\mu}}{2} \right) \right. \\ &\quad \left. - 9\hat{M}_D \left(\gamma + 2 \log 2 + \log \frac{\hat{\mu}}{2} \right) \right]. \end{aligned} \quad (46)$$

The second equation gives

$$\begin{aligned} \hat{m}_D^2 + \hat{m}_D^3 \left(\gamma + \frac{\pi^2}{3} + \log \frac{\hat{\mu}}{2} - \frac{8}{3} - \frac{4 \log 2}{3} \right) \\ = \frac{\lambda}{4\pi^2} \left[2 - 3\hat{M}_D + 3\hat{M}_D^2 - 8\hat{m}_q^2 - \hat{m}_D^2(1 + 8 \log 2) \right. \\ \left. - 6\hat{m}_D \hat{M}_D \left(\gamma + \log \frac{\hat{\mu}}{2} \right) \right. \\ \left. + \hat{m}_D \left(1.1753831 + 2 \log \hat{m}_D + \log \frac{\hat{\mu}}{2} \right) \right]. \end{aligned} \quad (47)$$

Finally, the third equation gives

$$\begin{aligned} \hat{M}_D^2 + 2\hat{M}_D^3 \left(\gamma + \log \frac{\hat{\mu}}{2} \right) \\ = \frac{\lambda}{4\pi^2} \left[1 - \frac{1}{2} \hat{m}_D + \hat{m}_D \hat{M}_D - \frac{1}{2} \hat{m}_D^2 \left(\gamma + \log \frac{\hat{\mu}}{2} \right) \right. \\ \left. + 8\hat{m}_q^2 \left(\gamma + 2 \log 2 + \log \frac{\hat{\mu}}{2} \right) \right. \\ \left. - 3\hat{M}_D^2 \left(4 \log 2 + 3\gamma + 3 \log \frac{\hat{\mu}}{2} + \frac{1}{2} \right) \right. \\ \left. + \hat{M}_D \left(0.677386934 + 2 \log \hat{M}_D + \log \frac{\hat{\mu}}{2} \right) \right]. \end{aligned} \quad (48)$$

We find that, similar to the DRG scheme, \hat{m}_q in Eqs. (47) and (48) can be written in terms of \hat{M}_D and \hat{m}_D by using (46). By numerically solving these three equations simultaneously, we obtain the gap equation solutions, $\hat{m}_q^{\text{gap}}(\lambda, \hat{\mu})$, $\hat{m}_D^{\text{gap}}(\lambda, \hat{\mu})$, and $\hat{M}_D^{\text{gap}}(\lambda, \hat{\mu})$.

In Fig. 1, we compare numerical solution of quark, gluon, and scalar gap equations in the RDR scheme to the result obtained using the DRG scheme. In these three panels, the results are obtained using the central value of the renormalization scale, $\hat{\mu} = 1$, and are scaled

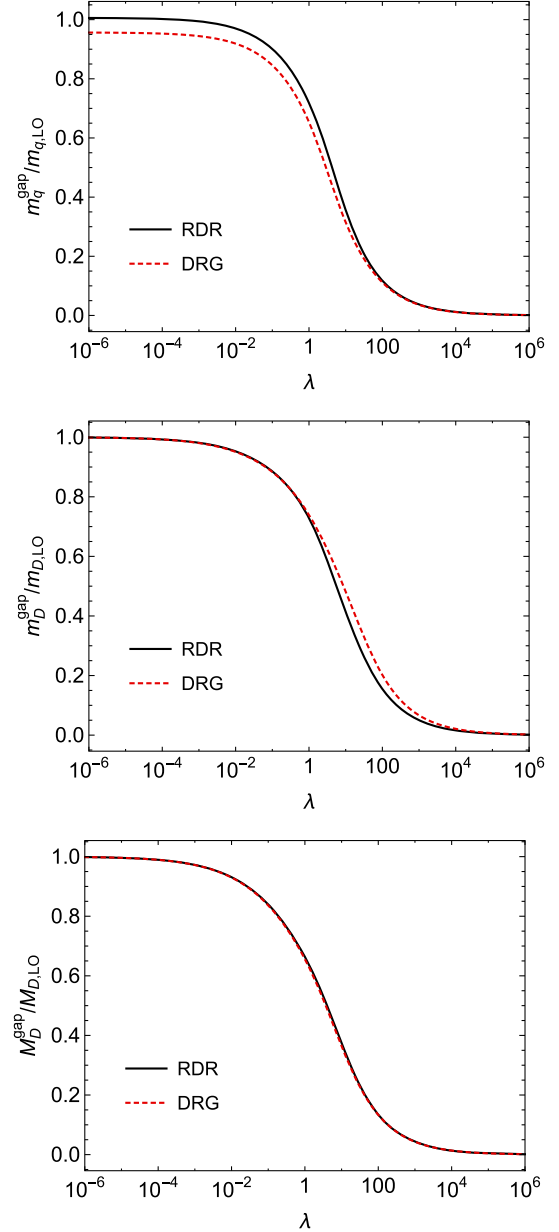


FIG. 1. Comparisons of the numerical solution of gap equations in the RDR and DRG schemes for m_q , m_D , and M_D as a function of λ with $\hat{\mu} = 1$. In each panel, the results are scaled by their corresponding leading-order weak-coupling limits.

by their corresponding leading-order weak-coupling limits. The red line is the result obtained using the RDR scheme, and the black dotted line is the result obtained using the DRG scheme. As one can see from Fig. 1, the results obtained in these two schemes are numerically similar to each other. At the central value $\mu = 2\pi T$, for the quark mass, the RDR result is slightly higher than the DRG result when $\lambda \rightarrow 0$ ¹; for the gluon mass, the RDR result is a little lower than the DRG result at intermediate λ ; for the scalar mass, the two results are nearly identical.

VI. THERMODYNAMIC FUNCTIONS IN THE RDR SCHEME

The NLO HTLpt-resummed free energy in the RDR scheme can be obtained by evaluating the NLO thermodynamic potential (41) at the solution of the gap equations (45),

$$\mathcal{F}_{\text{NLO}}^{\text{RDR}} = \Omega_{\text{NLO}}^{\text{RDR}}(T, \lambda, m_D^{\text{gap}}, M_D^{\text{gap}}, m_q^{\text{gap}}, \delta = 1). \quad (49)$$

The pressure, entropy density, and energy density can be obtained using

$$\begin{aligned} \mathcal{P} &= -\mathcal{F}, \\ \mathcal{S} &= -\frac{d\mathcal{F}}{dT}, \\ \mathcal{E} &= \mathcal{F} - T\frac{d\mathcal{F}}{dT}. \end{aligned} \quad (50)$$

In SYM_{4,4} these three quantities satisfy

$$\frac{\mathcal{P}}{\mathcal{P}_{\text{ideal}}} = \frac{\mathcal{S}}{\mathcal{S}_{\text{ideal}}} = \frac{\mathcal{E}}{\mathcal{E}_{\text{ideal}}}, \quad (51)$$

since λ is temperature independent.

A. Numerical results

In Fig. 2, we present a comparison of our NLO HTLpt result in the RDR and DRG schemes with the next-to-leading approximation (NLA) result of Blaizot, Iancu, Kraemmer, and Rebhan (BIKR) [71]. The green, blue, and cyan dashed/dotted lines represent the strict perturbation theory result given in Eq. (1), truncated at order λ , $\lambda^{3/2}$, λ^2 (including the logarithmic term), respectively. The orange dashed line is the strong coupling result given in Eq. (2). The purple dot-dashed line is the result of a generalized Padé approximant which is constructed based on Eqs. (1) and (2) [37]. The black and blue lines with a shaded bands are the NLO HTLpt result in the RDR and DRG schemes,

¹The gap equation solution for m_q does not approach its perturbative limit when λ approaches to zero in both schemes.

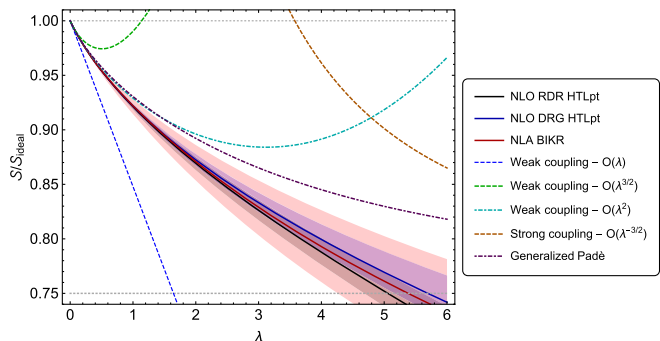


FIG. 2. Comparison of the NLO scaled entropy density obtained in the RDR scheme, the DRG scheme, and the prior NLA work of Blaizot, Iancu, Kraemmer, and Rebhan (BIKR) [71]. A detailed description of the various lines can be found in the text.

respectively. The bands correspond to variation of $\hat{\mu}$ in the range $1/2 \leq \hat{\mu} \leq 2$ and the solid lines correspond to $\hat{\mu} = 1$. Finally, the red line with a shaded band is the NLO BIKR result with the bands and line corresponding to scale variation and central value.

As Fig. 2 demonstrates, the DRG and RDR schemes result in similar predictions for $\lambda \lesssim 6$; however, both are below the generalized Padé which is constructed using the full order λ^2 and $\lambda^2 \log \lambda$ coefficients. Since the DRG scheme breaks supersymmetry, the RDR result should be taken as the correct NLO HTLpt result. In comparison with the BIKR result, which made use of the DRG scheme, we see that it is also in agreement to within a few percent for $\lambda \lesssim 6$.

In Fig. 3, we present a similar comparison, but for smaller λ in order to see the differences more clearly. The various strict perturbative results in this figure are the same as in Fig. 2. As can be seen from this figure, there is excellent agreement between the BIKR result and RDR NLO HTLpt in this coupling range. The generalized Padé approximant, however, only overlaps with both resummed results for $\lambda \lesssim 0.5$.

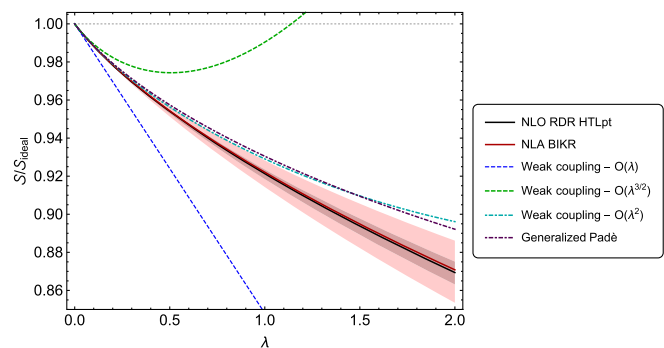


FIG. 3. Comparison of our NLO result for the scaled entropy density in the RDR scheme with prior results for small λ . Lines are the same as in Fig. 2.

VII. CONCLUSIONS

In this work, we obtained the LO and NLO HTLpt resummed thermodynamic potential in $\text{SYM}_{4,4}$ using the RDR regularization scheme. We then analytically and numerically compared the RDR result to the result obtained in the DRG scheme. From the analytical perspective, we found that differences emerged only in finite contributions, while the divergences were unaffected. This causes only a small change compared to DRG HTLpt result, which can be seen from the figures presented in Sec. VI A. Importantly, we found that, when expanded in strict perturbation theory, both schemes gave the same results for the coefficients of all terms contributing at orders λ , $\lambda^{3/2}$, and $\lambda^2 \log \lambda$, while at order λ^2 we found a weak residual regularization scheme dependence.

The results reported herein provide an important cross check of the coefficient of the order $\lambda^2 \log \lambda$ term in the free energy, independently confirming our prior result for this coefficient, which was obtained in Refs. [36,37]. The differences at order λ^2 are not yet conclusive; however, since in both the RDR and DRG schemes we have only performed a two-loop HTLpt calculation and a three-loop calculation is needed to properly fix this coefficient. Such a calculation was performed in strict perturbation theory in Refs. [36,37]. It would be interesting to extend the RDR HTLpt calculation to three-loop order in order to see how well it performs at large coupling; however, we first plan to complete the computation of the order $\lambda^{5/2}$ coefficient using effective field theory methods since this calculation is somewhat more manageable.

ACKNOWLEDGMENTS

We thank Jens O. Andersen for discussions and comments. Q.D. was supported by the Guangdong Major Project of Basic and Applied Basic Research No. 2020B0301030008 and the Natural Science Foundation of China Project No. 11935007. M.S. and U.T. were supported by the U.S. Department of Energy Award No. DE-SC0013470.

APPENDIX A: HTLPT FEYNMAN RULES FOR $\text{SYM}_{4,4}$ IN THE RDR SCHEME

In this Appendix, we will present the RDR scheme HTLpt Feynman rules for $\text{SYM}_{4,4}$ in Minkowski space. In Minkowski space, the momentum is denoted by $p = (p_0, \mathbf{p})$ and satisfies $p \cdot q = p_0 q_0 - \mathbf{p} \cdot \mathbf{q}$. The four-vector n^μ specifies the thermal rest frame and in the local rest frame of the plasma given by $n = (1, \mathbf{0})$.

We begin by noting that, since all ultraviolet divergences which are generated from the HTLpt reorganization are all canceled by systematically derivable counterterms, we only need to consider the leading order contributions to the gluon, quark, and scalar masses,

$$m_{D,\text{LO}}^2 = 2\lambda T^2, \quad M_{D,\text{LO}}^2 = \lambda T^2, \quad m_{q,\text{LO}}^2 = \frac{\lambda T^2}{2}, \quad (\text{A1})$$

which have been given previously in Refs. [48].

1. HTLpt gluon polarization tensor

In $\text{SYM}_{4,4}$, for massless bosons and fermions, the gluon polarization tensor in HTL limit can be expressed as

$$\Pi^{\mu\nu}(p) = m_D^2 [\mathcal{T}^{\mu\nu}(p, -p) - n^\mu n^\nu], \quad (\text{A2})$$

where we have introduced a rank-two tensor $\mathcal{T}^{\mu\nu}(p, q)$, which is defined only when $p + q = 0$,

$$\mathcal{T}^{\mu\nu}(p, -p) \equiv \left\langle y^\mu y^\nu \frac{p \cdot n}{p \cdot y} \right\rangle_{\hat{y}}. \quad (\text{A3})$$

The angular brackets represent an average over the spatial direction of the lightlike vector y . The tensor $\mathcal{T}^{\mu\nu}$ is symmetric in μ and ν , and satisfies the ‘‘Ward identity,’’

$$p_\mu \mathcal{T}^{\mu\nu}(p, -p) = (p \cdot n) n^\nu. \quad (\text{A4})$$

As a result, the polarization tensor $\Pi^{\mu\nu}$ is also symmetric in μ and ν and satisfies

$$\begin{aligned} p_\mu \Pi^{\mu\nu}(p) &= 0, \\ g_{\mu\nu} \Pi^{\mu\nu}(p) &= -m_D^2. \end{aligned} \quad (\text{A5})$$

The gluon polarization tensor can also be expressed in terms of two scalar functions, the transverse and longitudinal polarization functions Π_T and Π_L , which can be written as

$$\begin{aligned} \Pi_T(p) &= \frac{1}{D-2} (\delta^{ij} - \hat{p}^i \hat{p}^j) \Pi^{ij}(p), \\ \Pi_L(p) &= -\Pi^{00}(p), \end{aligned} \quad (\text{A6})$$

where $\hat{\mathbf{p}} = \mathbf{p}/|\mathbf{p}|$ is the unit vector in the direction of \mathbf{p} . The gluon polarization tensor can be expressed in terms of these two functions,

$$\Pi^{\mu\nu}(p) = -\Pi_T(p) T_p^{\mu\nu} - \frac{1}{n_p^2} \Pi_L(p) L_p^{\mu\nu}, \quad (\text{A7})$$

with

$$\begin{aligned} T_p^{\mu\nu} &= g^{\mu\nu} - \frac{p^\mu p^\nu}{p^2} - \frac{n_p^\mu n_p^\nu}{n_p^2}, \\ L_p^{\mu\nu} &= \frac{n_p^\mu n_p^\nu}{n_p^2}. \end{aligned} \quad (\text{A8})$$

The four-vector n_p^μ appearing above is defined by

$$n_p^\mu = n^\mu - \frac{n \cdot p}{p^2} p^\mu, \quad (\text{A9})$$

which satisfies $p \cdot n_p = 0$ and $n_p^2 = 1 - (n \cdot p)^2/p^2$. As a consequence, Eq. (A5) reduces to

$$(D-2)\Pi_T(p) + \frac{1}{n_p^2}\Pi_L(p) = m_D^2. \quad (\text{A10})$$

In the HTL limit, the polarization functions $\Pi_T(p)$ and $\Pi_L(p)$ can be written in terms of \mathcal{T}^{00} ,

$$\begin{aligned} \Pi_T(p) &= \frac{m_D^2}{(D-2)n_p^2} [\mathcal{T}^{00}(p, -p) - 1 + n_p^2], \\ \Pi_L(p) &= m_D^2 [1 - \mathcal{T}^{00}(p, -p)]. \end{aligned} \quad (\text{A11})$$

Note that, it is crucial to take the angular average in $d-1 = 3-2\epsilon$ in (A3), and then analytically continue to $d-1 = 3$ only after all poles in ϵ have been canceled. The expression for \mathcal{T}^{00} is

$$\mathcal{T}^{00}(p, -p) = \frac{\omega(\epsilon)}{2} \int_{-1}^1 dc (1-c^2)^{-\epsilon} \frac{p_0}{p_0 - |\mathbf{p}|c}, \quad (\text{A12})$$

where the weight function $\omega(\epsilon)$ is given by

$$\omega(\epsilon) = \frac{\Gamma(2-2\epsilon)}{\Gamma^2(1-\epsilon)} 2^{2\epsilon} = \frac{\Gamma(\frac{3}{2}-\epsilon)}{\Gamma(\frac{3}{2})\Gamma(1-\epsilon)}. \quad (\text{A13})$$

In the imaginary-time formalism, $\mathcal{T}^{00}(p, -p)$ can be expressed as

$$\mathcal{T}_P = \left\langle \frac{P_0^2}{P_0^2 + p^2 c^2} \right\rangle_c, \quad (\text{A14})$$

where the angular brackets represent an average over c defined by

$$\langle f(c) \rangle_c \equiv \omega(\epsilon) \int_0^1 dc (1-c^2)^{-\epsilon} f(c). \quad (\text{A15})$$

The definition of the gluon self energy in Eq. (A2) is the same as in QCD in Ref. [16] up to the definition of m_D . The HTLpt three-gluon vertex, four-gluon vertex, and ghost-gluon vertex are also similar C [48].

2. HTLpt gluon propagator

The HTLpt Feynman rule for the gluon propagator is

$$i\delta^{ab} \Delta_{\mu\nu}(p), \quad (\text{A16})$$

where a and b are adjoint color indices and

$$\begin{aligned} \Delta^{\mu\nu}(p) &= [-\Delta_T(p)g^{\mu\nu} + \Delta_X(p)n^\mu n^\nu] \\ &\quad - \frac{n \cdot p}{p^2} \Delta_X(p)(p^\mu n^\nu + n^\mu p^\nu) \\ &\quad + \left[\Delta_T(p) + \frac{(n \cdot p)^2}{p^2} \Delta_X(p) - \frac{\xi}{p^2} \right] \frac{p^\mu p^\nu}{p^2}, \end{aligned} \quad (\text{A17})$$

where Δ_T and Δ_L are the transverse and longitudinal propagators, respectively, and defined by

$$\begin{aligned} \Delta_T(p) &= \frac{1}{p^2 - \Pi_T(p)}, \\ \Delta_L(p) &= \frac{1}{-n_p^2 p^2 + \Pi_L(p)}, \end{aligned} \quad (\text{A18})$$

and $\Delta_X(p)$ is defined as

$$\Delta_X(p) = \Delta_L(p) + \frac{1}{n_p^2} \Delta_T(p). \quad (\text{A19})$$

3. HTLpt quark self energy, propagator, and counterterm

The HTLpt quark self energy is

$$\Sigma(p) = m_q^2 \mathcal{T}(p), \quad (\text{A20})$$

where we have suppressed the trivial Kronecker deltas and

$$\mathcal{T}^\mu(p) \equiv \left\langle \frac{y^\mu}{p \cdot y} \right\rangle_{\hat{y}}, \quad (\text{A21})$$

Similar to the gluon polarization tensor, the angular average in \mathcal{T}^μ can be written as

$$\mathcal{T}^\mu(p) = \frac{\omega(\epsilon)}{2} \int_{-1}^1 dc (1-c^2)^{-\epsilon} \frac{y^\mu}{p_0 - |\mathbf{p}|c}. \quad (\text{A22})$$

As was the case with the gluonic self energy, the quark self energy (A20) is the same as in QCD [17] up to the definition of m_q and taking into account the four Majorana fermions which are indexed by i . This will also occur in the HTLpt quark propagator, quark-gluon three vertex, and quark-gluon four vertex in SYM_{4,4} [48].

The HTLpt Feynman rule for the quark propagator is

$$i\delta^{ab} \delta^{ij} S(p), \quad (\text{A23})$$

where i, j index the four independent Majorana fermions and

$$S(p) = \frac{1}{\not{p} - \Sigma(p)} = \frac{1}{\mathcal{A}(p)}, \quad (\text{A24})$$

where $\mathcal{A}_\mu(p) = (\mathcal{A}_0(p), \mathcal{A}_s(p)\hat{\mathbf{p}})$ with

$$\begin{aligned} \mathcal{A}_0(p) &= p_0 - \frac{m_q^2}{p_0} \mathcal{T}_p, \\ \mathcal{A}_s(p) &= |\mathbf{p}| + \frac{m_q^2}{|\mathbf{p}|} [1 - \mathcal{T}_p]. \end{aligned} \quad (\text{A25})$$

The insertion of an HTL quark counterterm into a quark propagator corresponds to

$$i\delta^{ab} \delta^{ij} \Sigma(p). \quad (\text{A26})$$

4. HTLpt scalar self energy, propagator, and counterterm

The HTL scalar self energy can be expressed as

$$\mathcal{P}_{ab}^{AB}(p) = \delta_{ab} \delta^{AB} \lambda T^2, \quad (\text{A27})$$

and the corresponding Feynman rule for the scalar propagator is

$$i\delta^{ab} \delta^{AB} \Delta_s(p), \quad (\text{A28})$$

where

$$\Delta_s(p) = \frac{1}{p^2 - M_D^2}. \quad (\text{A29})$$

The insertion of an HTL scalar counterterm into a scalar propagator corresponds to

$$-i\delta^{ab} \delta^{AB} \mathcal{P}_{aa}^{AA}(p). \quad (\text{A30})$$

5. HTLpt quark-gluon vertex

The quark-gluon vertex with incoming quark momentum r , incoming gluon momentum p , and outgoing quark momentum q , Lorentz index μ , and color indices b, a, c is

$$\begin{aligned} \Gamma_{abc}^{\mu,ij}(p, q, r) &= -gf_{abc} \delta^{ij} [\gamma^\mu + m_q^2 \tilde{\mathcal{T}}^\mu(p, q, r)] \\ &= -gf_{abc} \delta^{ij} \Gamma^\mu(p, q, r). \end{aligned} \quad (\text{A31})$$

The rank-one tensor $\tilde{\mathcal{T}}^\mu$ is only defined for $p + r - q = 0$

$$\tilde{\mathcal{T}}^\mu(p, q, r) \equiv \left\langle y^\mu \left(\frac{\not{y}}{(y \cdot r)(y \cdot q)} \right) \right\rangle_{\hat{y}}, \quad (\text{A32})$$

and is even under the permutation of q and r . It satisfies

$$p_\mu \tilde{\mathcal{T}}^\mu(p, q, r) = \mathcal{T}(r) - \mathcal{T}(q). \quad (\text{A33})$$

The quark-gluon vertex therefore satisfies the Ward identity,

$$p_\mu \Gamma^\mu(p, q, r) = S^{-1}(q) - S^{-1}(r). \quad (\text{A34})$$

6. HTLpt quark-gluon four vertex

The quark-gluon four vertex with incoming quark momentum r , outgoing gluon momentum p, q , and outgoing quark momentum s is

$$\Gamma_{abcd}^{\mu\nu,ij}(p, q, r, s) = -ig^2 \delta^{ij} m_q^2 \tilde{\mathcal{T}}_{abcd}^{\mu\nu}(p, q, r, s), \quad (\text{A35})$$

and satisfies

$$\delta^{ij} \delta^{ad} \delta^{bc} \Gamma_{abcd,ij}^{\mu\nu}(p, q, r, s) = -4ig^2 N_c d_A \Gamma^{\mu\nu}(p, q, r, s), \quad (\text{A36})$$

where

$$\begin{aligned} \Gamma^{\mu\nu}(p, q, r, s) &= m_q^2 \left\langle y^\mu y^\nu \left(\frac{1}{y \cdot r} + \frac{1}{y \cdot s} \right) \right. \\ &\quad \left. \times \frac{\not{y}}{[y \cdot (r-p)][y \cdot (s+p)]} \right\rangle. \end{aligned} \quad (\text{A37})$$

This tensor is symmetric in μ and ν , and satisfies the Ward identity,

$$p_\mu \Gamma^{\mu\nu}(p, q, r, s) = \Gamma^\nu(q, r-p, s) - \Gamma^\nu(q, r, s+p). \quad (\text{A38})$$

7. HTLpt four scalar vertex

The four-scalar vertex is

$$\begin{aligned} \Gamma_{abcd}^{ABCD}(p, q, r, s) &= -ig^2 [f_{abef} f_{cde} (\delta^{AC} \delta^{BD} - \delta^{AD} \delta^{BC}) \\ &\quad + f_{ace} f_{bde} (\delta^{AB} \delta^{CD} - \delta^{AD} \delta^{BC}) \\ &\quad + f_{ade} f_{bce} (\delta^{AB} \delta^{CD} - \delta^{AC} \delta^{BD})]. \end{aligned} \quad (\text{A39})$$

It satisfies

$$\delta^{bd} \delta^{ac} \delta^{AC} \delta^{BD} \Gamma_{abcd}^{ABCD}(p, q, r, s) = (-ig^2)(60N_c d_A). \quad (\text{A40})$$

8. HTLpt scalar-gluon three vertex

The scalar-gluon vertex with incoming scalar momentum r , incoming gluon momentum p , and outgoing scalar momentum q is

$$\Gamma_{abc}^{\mu,AB}(p, q, r) = gf_{abc} \delta^{AB} (r+q)^\mu. \quad (\text{A41})$$

9. HTLpt scalar-gluon four vertex

The scalar-gluon four vertex is independent of the direction of the momentum and can be expressed as

$$\Gamma_{abcde}^{\mu\nu,AB}(p, q, r, s) = -2ig^2 g^{\mu\nu} \delta^{AB} f_{adef} f_{bce}. \quad (\text{A42})$$

It satisfies

$$\delta^{ac} \delta^{bd} \delta^{AB} \Gamma_{abcde}^{\mu\nu, AB}(p, q, r, s) = (2ig^2)(6N_c d_A) g^{\mu\nu}. \quad (\text{A43})$$

10. HTLpt quark-scalar vertex

There are two types of quark-scalar vertices, the quark-scalar vertex and the quark-pseudoscalar vertex. This is due to the fact that there are two types of interactions between quarks and scalars (X_p), and between quarks and pseudo-scalars (Y_q) which are different. The quark-scalar vertex, with incoming scalar momentum p , incoming quark momentum r and outgoing quark momentum q , and their corresponding colors indexed by a, c, b , can be written as

$$\Gamma_{abc,ij}^{\mathbb{P}}(p, q, r) = -igf_{abc} \alpha_{ij}^{\mathbb{P}}. \quad (\text{A44})$$

The quark-pseudoscalar vertex can be written as

$$\Gamma_{abc,ij}^{\mathbb{Q}}(p, q, r) = gf_{abc} \beta_{ij}^{\mathbb{Q}} \gamma_5. \quad (\text{A45})$$

APPENDIX B: INTEGRALS REQUIRED IN THE HTLPT CALCULATION

The one-loop sum-integrals required for the SYM_{4,4} NLO HTLpt calculation were presented in Appendix B of Refs. [16,17]. We list them here for completeness.

$$\sum_P \frac{1}{P^2} = T^2 \left(\frac{\mu}{4\pi T} \right)^{2\epsilon} \frac{1}{12} \left[1 + \left(2 + 2 \frac{\zeta'(-1)}{\zeta(-1)} \right) \epsilon \right], \quad (\text{B1})$$

$$\sum_P \frac{1}{P^4} = \frac{1}{(4\pi)^2} \left(\frac{\mu}{4\pi T} \right)^{2\epsilon} \left[\frac{1}{\epsilon} + 2\gamma + \left(\frac{\pi^2}{4} - 4\gamma_1 \right) \epsilon \right], \quad (\text{B2})$$

$$\sum_P \frac{p^2}{P^4} = \frac{1}{8} T^2, \quad (\text{B3})$$

$$\sum_P \frac{p^2}{P^6} = \frac{1}{(4\pi)^2} \left(\frac{\mu}{4\pi T} \right)^{2\epsilon} \frac{3}{4} \left[\frac{1}{\epsilon} + 2\gamma - \frac{2}{3} \right], \quad (\text{B4})$$

$$\sum_{\{P\}} \frac{p^2}{P^6} = \frac{1}{(4\pi)^2} \left(\frac{\mu}{4\pi T} \right)^{2\epsilon} \frac{3}{4} \left[\frac{1}{\epsilon} + 2\gamma - \frac{2}{3} + 4 \log 2 \right], \quad (\text{B5})$$

$$\sum_P \frac{p^4}{P^8} = \frac{1}{(4\pi)^2} \left(\frac{\mu}{4\pi T} \right)^{2\epsilon} \frac{5}{8} \left[\frac{1}{\epsilon} + 2\gamma - \frac{16}{15} \right], \quad (\text{B6})$$

$$\sum_P \frac{1}{P^2 P^2} = \frac{1}{(4\pi)^2} \left(\frac{\mu}{4\pi T} \right)^{2\epsilon} 2 \left[\frac{1}{\epsilon} + 2\gamma + 2 + \left(4 + 4\gamma + \frac{\pi^2}{4} - 4\gamma_1 \right) \epsilon \right]. \quad (\text{B7})$$

Similarly, the one-loop sum-integrals which involve HTL function \mathcal{T}_P are given by

$$\sum_P \frac{\mathcal{T}_P}{P^4} = \frac{1}{(4\pi)^2} \left(\frac{\mu}{4\pi T} \right)^{2\epsilon} (-1) \left[\frac{1}{\epsilon} + 2\gamma + 2 \log 2 \right], \quad (\text{B8})$$

$$\sum_P \frac{\mathcal{T}_P}{P^2 P^2} = \frac{1}{(4\pi)^2} \left(\frac{\mu}{4\pi T} \right)^{2\epsilon} \left[2 \log 2 \left(\frac{1}{\epsilon} + 2\gamma \right) + 2 \log^2 2 + \frac{\pi^2}{3} \right], \quad (\text{B9})$$

$$\sum_P \frac{(\mathcal{T}_P)^2}{P^4} = \frac{1}{(4\pi)^2} \left(\frac{\mu}{4\pi T} \right)^{2\epsilon} \left(-\frac{2}{3} \right) \left[(1 + 2 \log 2) \times \left(\frac{1}{\epsilon} + 2\gamma \right) - \frac{4}{3} + \frac{22}{3} \log 2 + 2 \log^2 2 \right], \quad (\text{B10})$$

$$\sum_{\{P\}} \frac{\mathcal{T}_P}{P^2 P_0^2} = \frac{1}{(4\pi)^2} \left(\frac{\mu}{4\pi T} \right)^{2\epsilon} \left[\frac{1}{\epsilon^2} + 2(\gamma + 2 \log 2) \frac{1}{\epsilon} + \frac{\pi^2}{4} + 4 \log^2 2 + 8\gamma \log 2 - 4\gamma_1 \right]. \quad (\text{B11})$$

The two-loop sum-integrals required can be split into two types. The first type are related to bosonic momentum integrations,

$$\sum_{PQ} \frac{1}{P^2 Q^2 R^2} = 0, \quad (\text{B12})$$

$$\sum_{PQ} \frac{1}{P^2 Q^2 r^2} = \frac{T^2}{(4\pi)^2} \left(\frac{\mu}{4\pi T} \right)^{4\epsilon} \frac{1}{12} \left[\frac{1}{\epsilon} + 10 - 12 \log 2 + 4 \frac{\zeta'(-1)}{\zeta(-1)} \right], \quad (\text{B13})$$

$$\sum_{PQ} \frac{q^2}{P^2 Q^2 r^4} = \frac{T^2}{(4\pi)^2} \left(\frac{\mu}{4\pi T} \right)^{4\epsilon} \frac{1}{6} \left[\frac{1}{\epsilon} + \frac{8}{3} + 2\gamma + 2 \frac{\zeta'(-1)}{\zeta(-1)} \right], \quad (\text{B14})$$

$$\sum_{PQ} \frac{q^2}{P^2 Q^2 R^2 r^2} = \frac{T^2}{(4\pi)^2} \left(\frac{\mu}{4\pi T} \right)^{4\epsilon} \frac{1}{9} \left[\frac{1}{\epsilon} + 7.521 \right], \quad (\text{B15})$$

$$\sum_{PQ} \frac{P \cdot Q}{P^2 Q^2 r^4} = \frac{T^2}{(4\pi)^2} \left(\frac{\mu}{4\pi T} \right)^{4\epsilon} \left(-\frac{1}{8} \right) \left[\frac{1}{\epsilon} + \frac{2}{9} + 4 \log 2 + \frac{8}{3} \gamma + \frac{4}{3} \frac{\zeta'(-1)}{\zeta(-1)} \right]. \quad (\text{B16})$$

The second type are related to fermionic momentum integrations,

$$\sum_{\{PQ\}} \frac{1}{P^2 Q^2 R^2} = 0, \quad (\text{B17})$$

$$\sum_{\{PQ\}} \frac{1}{P^2 Q^2 r^2} = \frac{T^2}{(4\pi)^2} \left(\frac{\mu}{4\pi T} \right)^{4\epsilon} \left(-\frac{1}{6} \right) \left[\frac{1}{\epsilon} + 4 - 2 \log 2 + 4 \frac{\zeta'(-1)}{\zeta(-1)} \right], \quad (\text{B18})$$

$$\oint_{\{PQ\}} \frac{q^2}{P^2 Q^2 r^4} = \frac{T^2}{(4\pi)^2} \left(\frac{\mu}{4\pi T} \right)^{4\epsilon} \left(-\frac{1}{12} \right) \left[\frac{1}{\epsilon} + \frac{11}{3} + 2\gamma - 2 \log 2 + 2 \frac{\zeta'(-1)}{\zeta(-1)} \right], \quad (\text{B19})$$

$$\oint_{\{PQ\}} \frac{P \cdot Q}{P^2 Q^2 r^4} = \frac{T^2}{(4\pi)^2} \left(\frac{\mu}{4\pi T} \right)^{4\epsilon} \left(-\frac{1}{36} \right) \times \left[1 - 6\gamma + 6 \frac{\zeta'(-1)}{\zeta(-1)} \right], \quad (\text{B20})$$

$$\oint_{\{PQ\}} \frac{q^2}{P^2 Q^2 R^2 r^2} = \frac{T^2}{(4\pi)^2} \left(\frac{\mu}{4\pi T} \right)^{4\epsilon} \left(-\frac{1}{72} \right) \left[\frac{1}{\epsilon} - 7.002 \right], \quad (\text{B21})$$

$$\oint_{\{PQ\}} \frac{p^2}{P^2 Q^2 R^2 q^2} = \frac{T^2}{(4\pi)^2} \left(\frac{\mu}{4\pi T} \right)^{4\epsilon} \frac{5}{72} \left[\frac{1}{\epsilon} + 9.5667 \right], \quad (\text{B22})$$

$$\oint_{\{PQ\}} \frac{r^2}{P^2 Q^2 R^2 q^2} = \frac{T^2}{(4\pi)^2} \left(\frac{\mu}{4\pi T} \right)^{4\epsilon} \left(-\frac{1}{18} \right) \left[\frac{1}{\epsilon} + 8.1420 \right]. \quad (\text{B23})$$

In a similar manner, the two-loop sum-integrals involving \mathcal{T}_P can be split into two types. The first type are related to the bosonic momentum integrations,

$$\oint_{PQ} \frac{\mathcal{T}_R}{P^2 Q^2 r^2} = \frac{T^2}{(4\pi)^2} \left(\frac{\mu}{4\pi T} \right)^{4\epsilon} \left(-\frac{1}{48} \right) \left[\frac{1}{\epsilon^2} + \left(2 - 12 \log 2 + 4 \frac{\zeta'(-1)}{\zeta(-1)} \right) \frac{1}{\epsilon} - 19.83 \right], \quad (\text{B24})$$

$$\oint_{PQ} \frac{q^2 \mathcal{T}_R}{P^2 Q^2 r^4} = \frac{T^2}{(4\pi)^2} \left(\frac{\mu}{4\pi T} \right)^{4\epsilon} \left(-\frac{1}{576} \right) \left[\frac{1}{\epsilon^2} + \left(\frac{26}{3} - \frac{24}{\pi^2} - 92 \log 2 + 4 \frac{\zeta'(-1)}{\zeta(-1)} \right) \frac{1}{\epsilon} - 477.7 \right], \quad (\text{B25})$$

$$\oint_{PQ} \frac{(P \cdot Q) \mathcal{T}_R}{P^2 Q^2 r^4} = \frac{T^2}{(4\pi)^2} \left(\frac{\mu}{4\pi T} \right)^{4\epsilon} \left(-\frac{1}{96} \right) \left[\frac{1}{\epsilon^2} + \left(\frac{8}{\pi^2} + 4 \log 2 + 4 \frac{\zeta'(-1)}{\zeta(-1)} \right) \frac{1}{\epsilon} + 59.66 \right]. \quad (\text{B26})$$

The second type are related to the fermionic momentum integrations,

$$\oint_{\{PQ\}} \frac{\mathcal{T}_R}{P^2 Q^2 r^2} = \frac{T^2}{(4\pi)^2} \left(\frac{\mu}{4\pi T} \right)^{4\epsilon} \left(-\frac{1}{48} \right) \left[\frac{1}{\epsilon^2} + \left(2 + 12 \log 2 + 4 \frac{\zeta'(-1)}{\zeta(-1)} \right) \frac{1}{\epsilon} + 136.362 \right], \quad (\text{B27})$$

$$\oint_{\{PQ\}} \frac{q^2 \mathcal{T}_R}{P^2 Q^2 r^4} = \frac{T^2}{(4\pi)^2} \left(\frac{\mu}{4\pi T} \right)^{4\epsilon} \left(-\frac{1}{576} \right) \left[\frac{1}{\epsilon^2} + \left(\frac{26}{3} + 52 \log 2 + 4 \frac{\zeta'(-1)}{\zeta(-1)} \right) \frac{1}{\epsilon} + 446.438 \right], \quad (\text{B28})$$

$$\oint_{\{PQ\}} \frac{(P \cdot Q) \mathcal{T}_R}{P^2 Q^2 r^4} = \frac{T^2}{(4\pi)^2} \left(\frac{\mu}{4\pi T} \right)^{4\epsilon} \left(-\frac{1}{96} \right) \left[\frac{1}{\epsilon^2} + \left(4 \log 2 + 4 \frac{\zeta'(-1)}{\zeta(-1)} \right) \frac{1}{\epsilon} + 69.174 \right], \quad (\text{B29})$$

$$\oint_{\{PQ\}} \frac{(r^2 - p^2) \mathcal{T}_Q}{P^2 q^2 Q_0^2 R^2} = -\frac{T^2}{(4\pi)^2} \left(\frac{\mu}{4\pi T} \right)^{4\epsilon} \frac{1}{8} \left[\frac{1}{\epsilon^2} + \left(2 + 2\gamma + \frac{10}{3} \log 2 + 2 \frac{\zeta'(-1)}{\zeta(-1)} \right) \frac{1}{\epsilon} + 46.8757 \right]. \quad (\text{B30})$$

[1] J.-L. Gervais and B. Sakita, *Nucl. Phys.* **B34**, 632 (1971).
 [2] D. V. Volkov and V. P. Akulov, *Phys. Lett.* **46B**, 109 (1973).
 [3] V. P. Akulov and D. V. Volkov, *Theor. Math. Phys.* **18**, 28 (1974).
 [4] H. P. Nilles, *Phys. Rep.* **110**, 1 (1984).
 [5] S. P. Martin, *Adv. Ser. Dir. High Energy Phys.* **18**, 1 (1998).
 [6] J. M. Maldacena, *Adv. Theor. Math. Phys.* **2**, 231 (1998).

[7] S. S. Gubser, I. R. Klebanov, and A. A. Tseytlin, *Nucl. Phys.* **B534**, 202 (1998).
 [8] J. O. Andersen, E. Braaten, and M. Strickland, *Phys. Rev. Lett.* **83**, 2139 (1999).
 [9] J. P. Blaizot, E. Iancu, and A. Rebhan, *Phys. Rev. Lett.* **83**, 2906 (1999).
 [10] J. O. Andersen, E. Braaten, and M. Strickland, *Phys. Rev. D* **61**, 014017 (1999).

- [11] J. P. Blaizot, E. Iancu, and A. Rebhan, *Phys. Lett. B* **470**, 181 (1999).
- [12] J. O. Andersen, E. Braaten, and M. Strickland, *Phys. Rev. D* **61**, 074016 (2000).
- [13] J. P. Blaizot, E. Iancu, and A. Rebhan, *Phys. Rev. D* **63**, 065003 (2001).
- [14] A. Peshier, *Phys. Rev. D* **63**, 105004 (2001).
- [15] J. P. Blaizot, E. Iancu, and A. Rebhan, *Phys. Lett. B* **523**, 143 (2001).
- [16] J. O. Andersen, E. Braaten, E. Petitgirard, and M. Strickland, *Phys. Rev. D* **66**, 085016 (2002).
- [17] J. O. Andersen, E. Petitgirard, and M. Strickland, *Phys. Rev. D* **70**, 045001 (2004).
- [18] J. P. Blaizot, E. Iancu, and A. Rebhan, *Phys. Rev. D* **68**, 025011 (2003).
- [19] J. O. Andersen, M. Strickland, and N. Su, *Phys. Rev. Lett.* **104**, 122003 (2010).
- [20] J. O. Andersen, M. Strickland, and N. Su, *J. High Energy Phys.* **08** (2010) 113.
- [21] J. O. Andersen, L. E. Leganger, M. Strickland, and N. Su, *Phys. Lett. B* **696**, 468 (2011).
- [22] J. O. Andersen, L. E. Leganger, M. Strickland, and N. Su, *J. High Energy Phys.* **08** (2011) 053.
- [23] J. O. Andersen, L. E. Leganger, M. Strickland, and N. Su, *Phys. Rev. D* **84**, 087703 (2011).
- [24] N. Haque, M. G. Mustafa, and M. Strickland, *Phys. Rev. D* **87**, 105007 (2013).
- [25] N. Haque, M. G. Mustafa, and M. Strickland, *J. High Energy Phys.* **07** (2013) 184.
- [26] N. Haque, J. O. Andersen, M. G. Mustafa, M. Strickland, and N. Su, *Phys. Rev. D* **89**, 061701 (2014).
- [27] N. Haque, A. Bandyopadhyay, J. O. Andersen, M. G. Mustafa, M. Strickland, and N. Su, *J. High Energy Phys.* **05** (2014) 027.
- [28] J. O. Andersen, N. Haque, M. G. Mustafa, and M. Strickland, *Phys. Rev. D* **93**, 054045 (2016).
- [29] N. Haque and M. Strickland, *Phys. Rev. C* **103**, L031901 (2021).
- [30] S. C. Huot, S. Jeon, and G. D. Moore, *Phys. Rev. Lett.* **98**, 172303 (2007).
- [31] A. Czajka and S. Mrówczyński, *Acta Phys. Pol. B Proc. Suppl.* **7**, 145 (2014).
- [32] A. Fotopoulos and T. R. Taylor, *Phys. Rev. D* **59**, 061701 (1999).
- [33] C.-j. Kim and S.-J. Rey, *Nucl. Phys.* **B564**, 430 (2000).
- [34] M. A. Vazquez-Mozo, *Phys. Rev. D* **60**, 106010 (1999).
- [35] A. Nieto and M. H. G. Tytgat, [arXiv:hep-th/9906147](https://arxiv.org/abs/hep-th/9906147).
- [36] Q. Du, M. Strickland, and U. Tantary, *J. High Energy Phys.* **08** (2021) 064.
- [37] J. O. Andersen, Q. Du, M. Strickland, and U. Tantary, *Phys. Rev. D* **105**, 015006 (2022).
- [38] J. M. Luttinger and J. C. Ward, *Phys. Rev.* **118**, 1417 (1960).
- [39] G. Baym, *Phys. Rev.* **127**, 1391 (1962).
- [40] J. M. Cornwall, R. Jackiw, and E. Tomboulis, *Phys. Rev. D* **10**, 2428 (1974).
- [41] B. A. Freedman and L. D. McLerran, *Phys. Rev. D* **16**, 1169 (1977).
- [42] A. Arrizabalaga and J. Smit, *Phys. Rev. D* **66**, 065014 (2002).
- [43] J. O. Andersen and M. Strickland, *Phys. Rev. D* **71**, 025011 (2005).
- [44] J. O. Andersen, E. Braaten, and M. Strickland, *Phys. Rev. D* **63**, 105008 (2001).
- [45] J. O. Andersen and M. Strickland, *Phys. Rev. D* **64**, 105012 (2001).
- [46] J. O. Andersen and L. Kyllingstad, *Phys. Rev. D* **78**, 076008 (2008).
- [47] J. O. Andersen, M. Strickland, and N. Su, *Phys. Rev. D* **80**, 085015 (2009).
- [48] Q. Du, M. Strickland, U. Tantary, and B.-W. Zhang, *J. High Energy Phys.* **09** (2020) 038.
- [49] J. F. Ashmore, *Lett. Nuovo Cimento* **4**, 289 (1972).
- [50] C. G. Bollini and J. J. Giambiagi, *Nuovo Cim B* **12**, 20 (1972).
- [51] G. 't Hooft and M. Veltman, *Nucl. Phys.* **B44**, 189 (1972).
- [52] W. Siegel, *Phys. Lett.* **84B**, 193 (1979).
- [53] L. Brink, J. H. Schwarz, and J. Scherk, *Nucl. Phys.* **B121**, 77 (1977).
- [54] F. Gliozzi, J. Scherk, and D. I. Olive, *Nucl. Phys.* **B122**, 253 (1977).
- [55] L. V. Avdeev and A. A. Vladimirov, *Nucl. Phys.* **B219**, 262 (1983).
- [56] D. Capper, D. Jones, and P. Van Nieuwenhuizen, *Nucl. Phys.* **B167**, 479 (1980).
- [57] C. M. Bender and T. T. Wu, *Phys. Rev.* **184**, 1231 (1969).
- [58] C. M. Bender and T. T. Wu, *Phys. Rev. D* **7**, 1620 (1973).
- [59] W. Janke and H. Kleinert, *Phys. Rev. Lett.* **75**, 2787 (1995).
- [60] H. Kleinert and W. Janke, *Phys. Lett. A* **206**, 283 (1995).
- [61] W. A. Bardeen, A. J. Buras, D. W. Duke, and T. Muta, *Phys. Rev. D* **18**, 3998 (1978).
- [62] G. 't Hooft, *Nucl. Phys.* **B61**, 455 (1973).
- [63] S. Weinberg, *Phys. Rev. D* **8**, 3497 (1973).
- [64] P. Stevenson, *Nucl. Phys.* **B203**, 472 (1982).
- [65] G. P. Lepage, in *Theoretical Advanced Study Institute in Elementary Particle Physics* (1989), [arXiv:hep-ph/0506330](https://arxiv.org/abs/hep-ph/0506330).
- [66] F. Quevedo, S. Krippendorff, and O. Schlotterer, [arXiv:1011.1491](https://arxiv.org/abs/1011.1491).
- [67] M. Bertolini, SISSA—International School for Advanced Studies (2015), <https://people.sissa.it/~bertmat/susycourse.pdf>.
- [68] D. Yamada and L. G. Yaffe, *J. High Energy Phys.* **09** (2006) 027.
- [69] E. D'Hoker and D. H. Phong, in *Theoretical physics at the end of the twentieth century, Proceedings, Summer School, Banff, Canada, 1999* (1999), pp. 1–125, [arXiv:hep-th/9912271](https://arxiv.org/abs/hep-th/9912271).
- [70] S. Kovacs, *N = 4 supersymmetric Yang-Mills theory and the AdS / SCFT correspondence*, Ph.D. thesis, University of Rome “Tor Vergata”, 1999, [arXiv:hep-th/9908171](https://arxiv.org/abs/hep-th/9908171).
- [71] J. P. Blaizot, E. Iancu, U. Kraemmer, and A. Rebhan, *J. High Energy Phys.* **06** (2007) 035.